XAS spectroscopy and Multiple Scattering Theory

M. Benfatto

Laboratori Nazionali di Frascati dell'INFN – Frascati ITALY

Outline of the lessons

- **XAS and MS Theory**
- **Quantitative analysis of the XAS data: the low energy region**
- **XAS and Molecular Dynamics**
- **Time dependend data**

Absorption coefficient from core levels

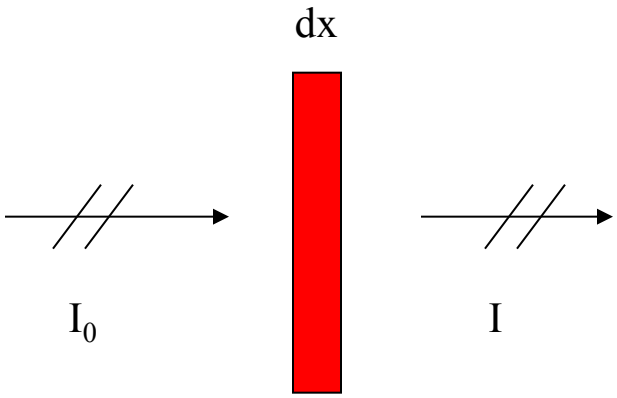

$$dI=\mu(E)\, I\, dx \longrightarrow I=I_0 e^{-\mu(E)x}$$

$\mu(E) = n_{ab}\, \sigma(E)$

E is in the X-ray energy range

Density of absorption medium

Photoabsorption cross section

There are other scattering processes
with and without energy loss

Physical process: excitation of core-level electron to continuum states

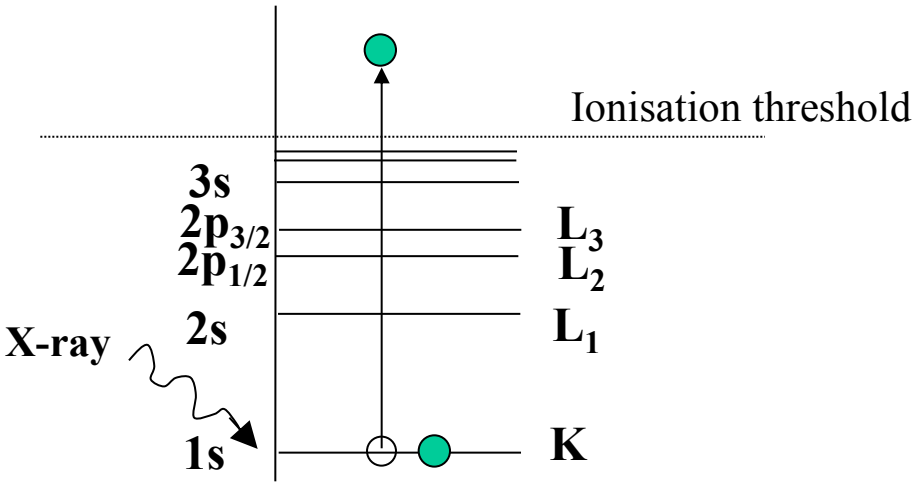

we use the Fermi "golden rule" to calculate the total cross-section of this process

we use the dipole approximation

$$\sigma(\omega) = 4\pi^2 \alpha\, \omega \sum_f \left| \langle \psi_f \left| \vec{\varepsilon} \cdot \vec{r} \right| \psi_c \rangle \right|^2 \delta(\omega - E_f + E_c)$$

Dipole approximation $\longleftrightarrow$ $\dfrac{\sigma_q(\omega)}{\sigma_d(\omega)} \approx \dfrac{1}{100}$

$\psi_f \longrightarrow$ w.f. in the final state

$\psi_c \longrightarrow$ core w.f. spatially localized

we use multiple scattering theory to get the final state w.f.

the core level is spatially localized - we only need the final state ψ_f in the absorbing site

MS Theory

It is a method to solve the Sch. Equation in real space and it does not need any particular symmetry. Introduced in the literature by K. H. Johnson since ’60-’70 to calculate bound states in small molecules

$$\left[-\nabla^2 + V(\vec{r})\right]\Psi(\vec{r}) = E\Psi(\vec{r})$$

$$V(\vec{r}) = V_c(\vec{r}) + V_{exc}(\vec{r})$$

Some approximation must be done – we use the HL potential within a quasi-particle scheme

$$V_c(\vec{r}) = \sum_j V^j(\vec{r} - R_j)$$

Sum of free atomic potential ⟷ cluster of atoms

Muffin-Tin approximation

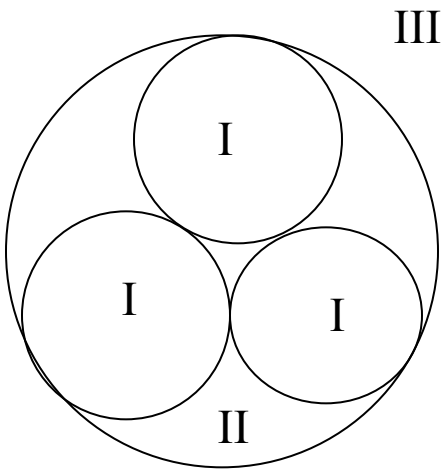

The space is divided in three regions

$$V_I(\vec{r}) = \sum_L V_L(r) Y_L(\hat{r}) \; ; \; L \equiv l,m$$

Only the L=0 is considered

$$V_{II}(\vec{r}) = V_{MT} = \frac{1}{\Omega_{II}} \int_{\Omega_{II}} V(\vec{r})\, d\vec{r}$$

V_{MT} is a constant value - The average is over the interstitial volume

V_{III} is a spherical average respect to the atomic cluster center - It depends to the physical problem to be solved.

We must solve the Sch. equation with this potential

The total w.f. can be written as:

$$\Psi = \sum_j \Psi_I^j + \Psi_{II} + \Psi_{III}$$

- In each atomic region (region I) the w.f. is developed into spherical harmonics:

$$\Psi_I^J(\vec{r}) = \sum_L B_L^J R_l^J(E;r) Y_L(\hat{r})$$

- V_{MT} is constant $\longrightarrow$ Ψ_{II} is a combination of Bessel and Neumann functions

In the outer sphere region (region III)

$$\Psi_{III} = \sum_{L,L'} [A_L^{III} f_l^{III}(kr_0)\delta_{LL'} + B_{LL'}^{III} g_{l'}^{III}(kr_0)] Y_{L'}(\hat{r}_0)$$

regular part

irregular part

center of the whole molecules

This is a very general expression - The asymptotic behavior of f_l and g_l allow us to go from bound to continuum states.

We impose the continuity of wave function Ψ and its first derivate at the border of the different regions

Compatibility equations between B_L^j coefficients

i) Eigen-values of the bounded molecular states
ii) w.f. in the various regions
iii) Spectroscopy quantities

we get this set of compatibility equations

$$B^i_L(\underline{L}) + t^i_l \sum_{j\neq i} \widetilde{G}^{ij}_{LL'} B^j_{L'}(\underline{L}) = -t^i_l J^{io}_{L\underline{L}} \Gamma_{\underline{L}}$$

valid for both bound and continuum states

$$\widetilde{G}^{ij}_{LL'} = G^{ij}_{LL'} - \sum_{L"} J^{i0}_{LL"} t^0_{l"} J^{oj}_{L"L'}$$

$$t^i_l = W[j_l, R^i_l] / W[-ih^+_l, R^i_l] = e^{i\delta^i_l} \sin\delta^i_l$$

$$W[f(x), g(x)] = f(x)\frac{d}{dx}g(x) - g(x)\frac{d}{dx}f(x)$$

corrections due to the OS sphere, region III

$$G^{ij}_{LL'} = -4\pi i \sum_{L"} i^{l"+l'-l} C^{L}_{L'L"} h^+_{l"}(kR_{ij}) Y_{L"}(\hat{R}_{ij})$$

$G^{ii}_{LL'} \equiv 0$

Gaunt coefficient

$J^{i0}_{L\underline{L}}$ ⟶ Exciting wave referred to site i

$$B_L^i(\underline{L}) + t_l^i \sum_{j \neq i} \tilde{G}_{LL'}^{ij} B_{L'}^j(\underline{L}) = -t_l^i J_{L\underline{L}}^{io} \Gamma_{\underline{L}}$$

The amplitude of the wave function at each atomic site i is formed by the one coming from the center plus all arriving from the other sites.

The model is a multiple scattering model for several centers with free propagation in the interstitial region

T. Tyson et al. Phys. Rev B46 5997 (1992)

We have also demonstrated that it is possible to eliminate the OS by changing the normalization – the so-called "extended continuum" scheme

bound states can be found as continuum resonances, in other words for $E > V_{MT}$ (it is a negative value) we can found all the possible states as continuum states

unique energy scale from the pre-edge to the EXAFS energy region

M. Benfatto et al. Phys. Rev B34 5774 (1986)
T. Tyson et al. Phys. Rev B46 5997 (1992)

We need to know the final state wave function at absorbing site 0 because of the localization of the core wave function

$$\sigma(\omega) \approx \sum_{\underline{L},L,m_\gamma,m_0} \left|B_L^0(\underline{L})\right|^2 \left|(R_L^0(\vec{r}_0) \mid r_0 Y_{lm_\gamma}(\hat{r}_0) \mid \phi_{l_0}^0(r_0) Y_{L_0}(\hat{r}_0))\right|^2$$

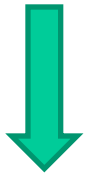

un-polarized photo-absorption cross section

it is convinient to define the matrix

$$T_a = \begin{pmatrix} t_l^0 & \cdots & 0 \\ \vdots & \ddots & \vdots \\ 0 & \cdots & t_l^n \end{pmatrix}$$

Optical theorem

$$\sum_{\underline{L}} [B_L^0(\underline{L})]^* [B_{L'}^0(\underline{L})] = \mathrm{Im}[(I - T_a \widetilde{G})^{-1} T_a]_{LL'}^{00}$$

$$\tau_{LL'}^{00} = [(I - T_a \widetilde{G})^{-1} T_a]_{LL'}^{00}$$

$$\begin{pmatrix} .. & & \widetilde{G}_{ij} \\ & (t_\ell^i)^{-1} & \\ \widetilde{G}_{ji} & & .. \end{pmatrix}^{-1}$$

scattering path operator – it contains all the structural and electronic information

$$\sigma(\omega) = -4\pi\alpha\hbar\omega \sum_{LL'} \mathrm{Im}[(M^*)_L^0 \tau_{LL'}^{00} M_{L'}^0]$$

$$M_L^0 = \int \phi_{L_0}^0(\vec{r})\, \hat{\varepsilon} \cdot \vec{r}\, R_L^0(\vec{r})\, d^3r$$

it is possible to separate the atomic contribution to the oscillating part

$$\sigma(E)=(l+1)\sigma_0^{l_0+1}(E)\,\chi^{l_0+1}(E)+l\,\sigma_0^{l_0-1}(E)\,\chi^{l_0-1}(E)$$

$$\chi^{l}(E)=\frac{1}{(2l+1)\sin^2\delta_l^0}\sum_m \mathrm{Im}\,\tau_{lmlm}^{00}$$

$$\sigma_0^l(E)=\frac{8\pi^2}{3}\alpha k(E+I_0)\sin^2\delta_l^0\left[\int_0^\infty r^3 R_l(r)\phi_{l_0}(r)\,dr\right]^2$$

atomic cross section - almost without structures and independent from the energy

Final angular momentum according dipole selection rule

$$l = l_0 \pm 1$$

Main ingredients

- Partition of the space in spheres
- Expansion theorem – use of the SA expansion
- Compatibility equations – scattering solution
- There is not any need to a basis set as done in other methods like DFT..

There is the possibility to overcome the MT approximation by introducing a suitable correction to both the propagators and the t-matrix

$$(T_a^i)^{-1} \rightarrow (T_a^i)^{-1} + T^{ii}$$

$$G^{ij} \rightarrow G^{ij} + T^{ij}$$

The scattering path operator can be calculated exactly or by series when the spectral radius ρ less than one

$$(\mathrm{I}-\mathrm{T_a G})^{-1}=\sum_{\mathrm{n=0}}(\mathrm{T_a G})^{\mathrm{n}}$$

$$\tau = T_a + T_a G T_a G T_a + T_a G T_a G T_a G T_a + ...$$

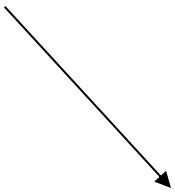

$$G^{ii}_{LL'} \equiv 0$$ we start from n=2

The size of the spectral radius depends by the energy

The interpretation in term of series is valid only if

$$\rho \leq 1$$

In general

$$\rho \xrightarrow[k\to\infty]{} 0 \qquad (t_1 \to 0)$$

$$\rho \xrightarrow[k\to 0]{} \infty \qquad (G \to \infty)$$

$$\begin{cases} \text{High energy} \rightarrow \sigma_0 \text{ or } \sigma_0 + \sigma_2 \\ \text{Low energy} \rightarrow \sigma_0 + \sigma_2 + \sigma_3 + ... \end{cases}$$

MS paths

$$\sigma_n = \sigma_0 \chi_n^l$$

σ_0 – smooth atomic contribution

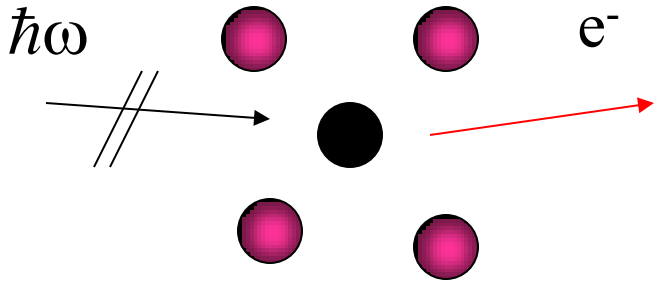

σ_2 – single diffusion – EXAFS region

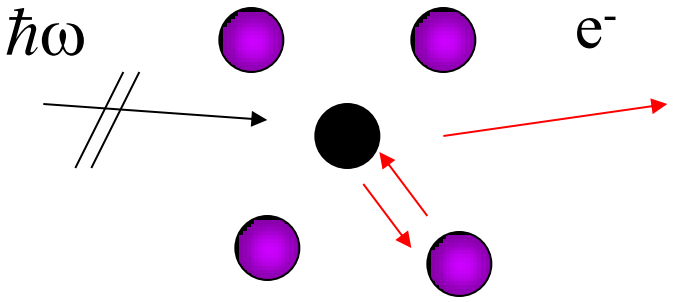

$$t_l^0 G t_l^i G t_l^0 \approx \frac{1}{(kR)^2}$$

σ_3 – double diffusion – high order correlation functions

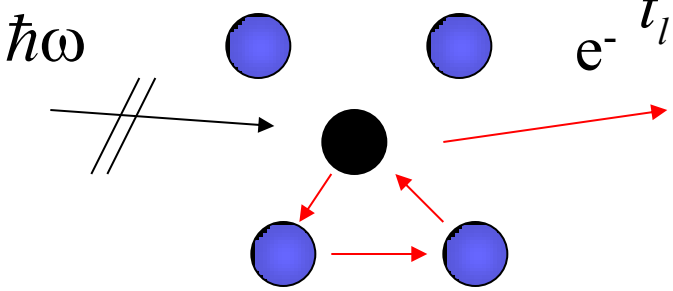

$$t_l^0 G t_l^i G t_{l'}^j G t_l^0 \approx \frac{1}{(kR_{tot})^3}$$

When we can develop in series all the structural information are contained in the structural factor

$$\chi^{l}(E) = 1 + \sum_{n=2} \chi^{l}_{n}(E)$$

$$\chi^{l}_{n}(E) = \frac{1}{(2l+1)\sin^{2}\delta^{0}_{l}} \sum_{m} \mathrm{Im}[(T_a G)^{n} T_a]^{00}_{lmlm}$$

partial contribution of order n coming from all process where the photoelectron is scattered n-1 time by the surrounding atoms before escaping to free space after returning to absorbing atom

The calculation of the EXAFS signal

$$\chi_2^l = \frac{1}{2l+1} \sum_{j \neq 0} \sum_{mm'l'} \mathrm{Im}\{ e^{2i\delta_l^0} G_{lml'm'}^{0j} t_{l'}^j G_{l'm'lm}^{j0} \}$$

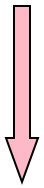

$$\chi_2^l = (-1)^l \sum_{j \neq 0} \sum_{l'} \mathrm{Im}\{ e^{2i\delta_l^0} (i)^{2l'+1} t_{l'}^j (2l'+1) H(l,l',kR_{j0}) \}$$

where

$$H(l,l',kR_{j0}) = \sum_{l''} (i)^{l''} (2l''+1) \begin{pmatrix} l & l' & l'' \\ 0 & 0 & 0 \end{pmatrix}^2 (h_{l''}^+(kR_{j0}))^2$$

All other signals can be derived in the same way by 3j, 6j, 9j symbols.

Plane wave approximation

$$(i)^l \, h_l^+(kR) \to \frac{e^{ikR}}{kR}$$

$$\chi_2^l = (-1)^l \sum_{j \neq 0} \mathrm{Im}\{e^{2i\delta_l^0} \, \frac{e^{2ikR_{j0}}}{(kR_{j0})^2} F_j(k)\}$$

$$F_j(k) = \frac{1}{k} \sum_l (i)^{2l+1} (2l+1) e^{i\delta_l^j} \, \sin\delta_l^j$$

The phase does not depend by the distance

some conclusions

- Core levels are spatially localized
- Every atom has a well defined core levels

site selectivity

The photoelectron probes the system

Strong interaction with the matter

Infomation beyond the pair correlation functions

We need to account for other physical processes

- inelastic excitations suffered by the photoelectron
- electronic excitations due to the creation on core-hole
- finite core hole width
- …….

They drain away amplitude from the elastic channel and must be included in any realistic calculation

finite lifetime of the photoelectron in the final state

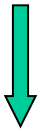

many-body treatment of the photoabsorption process

• we have generalized the MS theory to treat the case where several electronic configurations are present MC-MS theory

• we have also demonstrated that if just one electronic configuration dominates we can eliminate from the set all channels which give rise to similar inter-channels potential

• from many body to an effective one particle problem – it is convinient to use the Green function formalism

$$\sigma(E) \propto \mathrm{Im}\, G_{00}(E - I_c)$$

$$[\nabla^2 + E - V_c(\vec{r}) - \Sigma_{exc}(\vec{r}, E)] G^+_{00}(\vec{r}, \vec{r}', E) = \delta(\vec{r} - \vec{r}')$$

$$\Sigma_{exc}(\vec{r}, E) = V(\vec{r}, E) + i\Gamma(\vec{r}, E)$$

For a muffin-tin potential

$$G^+_{00}(\vec{r}, \vec{r}', E) = -k \sum_{L,L'} R^0_L(\vec{r}) \tau^{00}_{L,L'} R^0_{L'}(\vec{r}') + \sum_L R^0_L(\vec{r}) S^0_L(\vec{r}')$$

usual scattering path operator -complete equivalence between Green function and MS approaches

C.R. Natoli, M. Benfatto et al. Phys. Rev **B42** 1944(1990)
T. Tyson et al. Phys. Rev **B46** 5997(1992)
C.R. Natoli, M. Benfatto et al. Jour. Synch. Rad. **10** 26 (2003)

The use of complex potential automatically introduces a damping in the the elastic signal

$$G_{LL'}^{ij} \approx \frac{e^{ikR_{ij}}}{kR_{ij}}$$

If $k = k_r + i\, k_i$ we have a decreasing exponential

we choose the Hedin-Lundqvist (HL) potential extending its validity in to the atomic core region

it has an imaginary part that is able to reproduce the observed mean-free path in metal. This part starts at the plasmon energy

we see only few shells around the absorber typically 5-10 at the edge

Within some conditions the use of an optical potential is completely equivalent to a convolution of a real calculation with a Lorentzian function having a suitable energy dependent width

S K-edge in ZnS

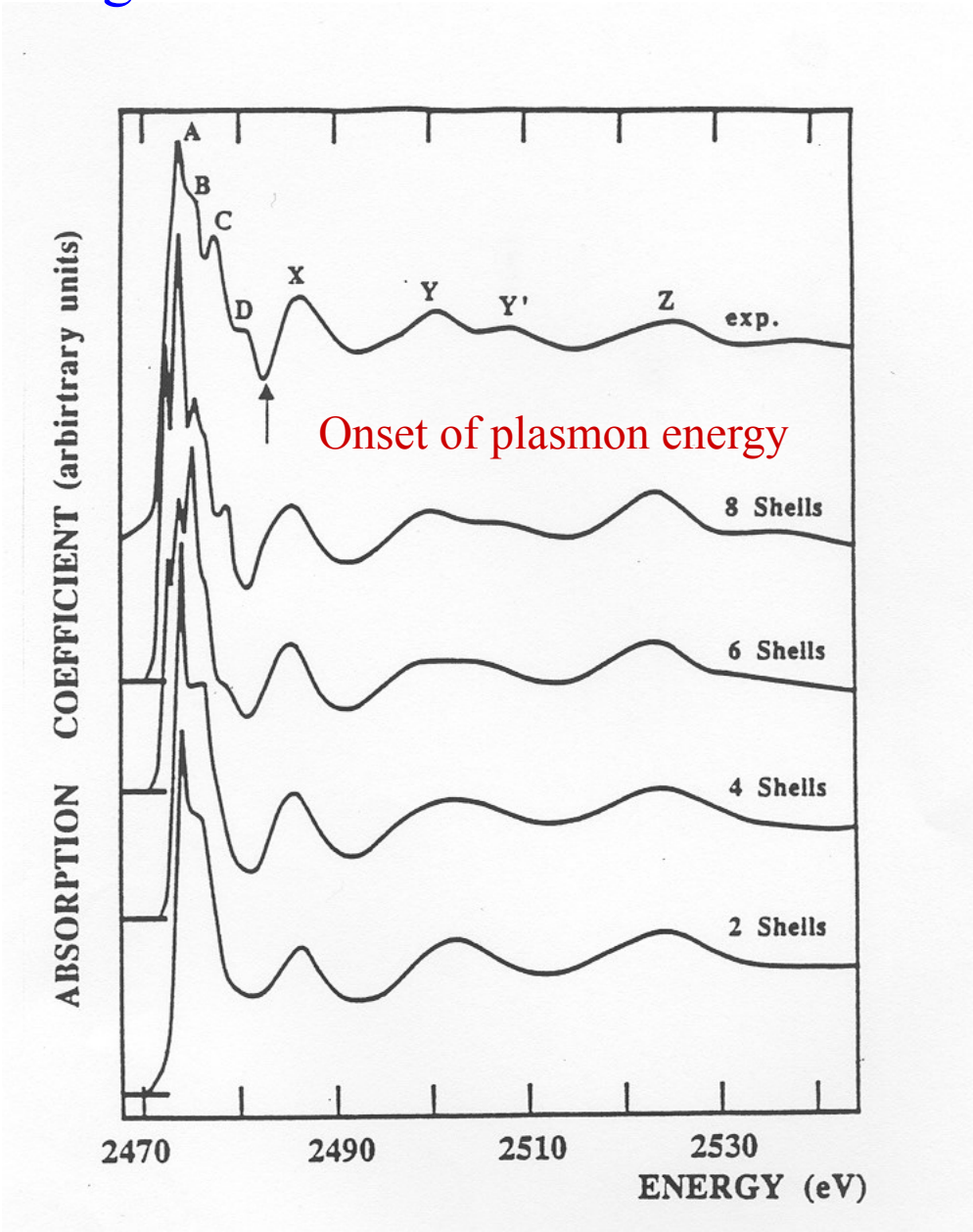

The cross section has been built shell by shell

How to get structural information

Methods essentially based on FT and the concept of phase transferability, normally they are limited to the first shell analysis and systems with negligible MS contribution

These methods use mainly the EXAFS part of the spectrum

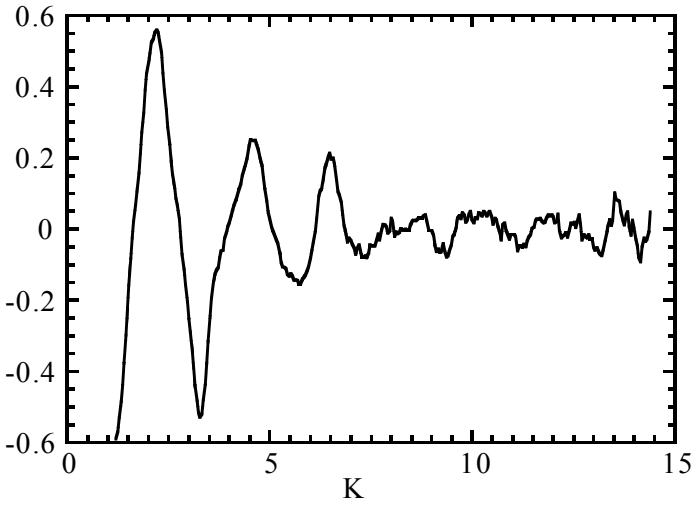

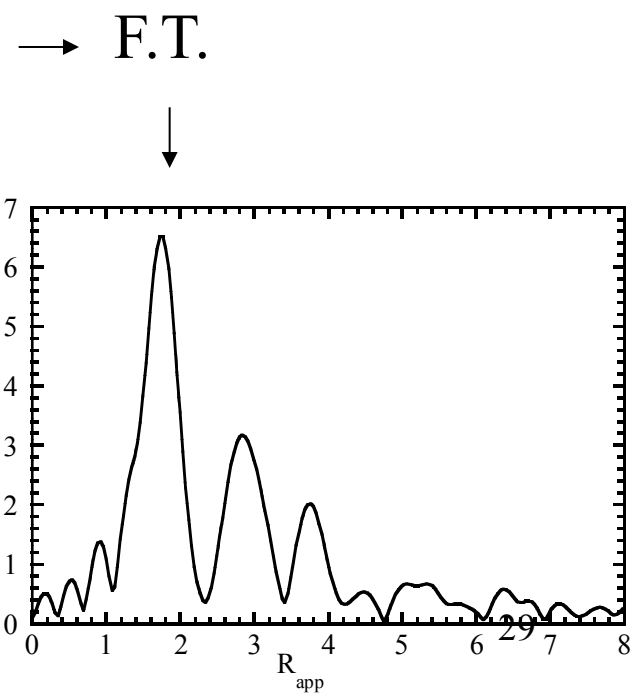

Other methods are based on fit procedure that use the MS approach to generate the theoretical MS series, i.e. χ_n many signals to be compared with exp. data. By moving bond lengths and angles those programs reach the best fit conditions in term of structural used parameters.

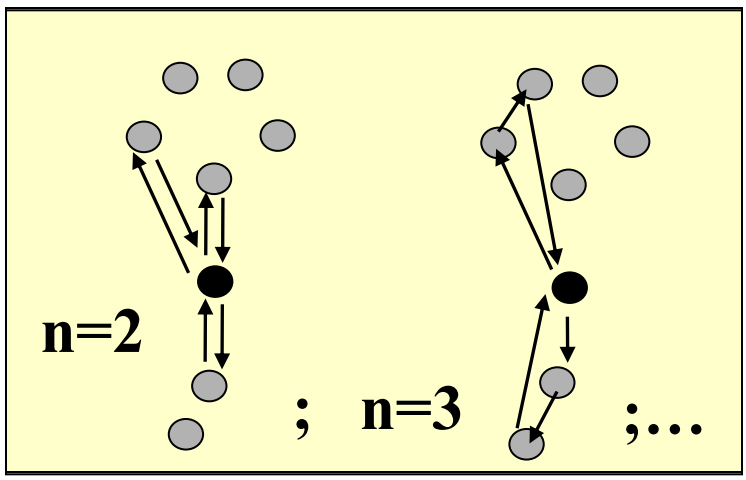

Feff --- EXCURVE

Normally the XANES energy region is used on the basis of qualitative manner

In 2001 we have developed a new method to use XANES (from edge to about 200 eV) as a source of **quantitative** structural information.

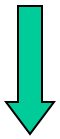

← Why?

Many XAS spectra "contain" most of the structural information in XANES energy region, in particular biological samples because the scattering power decreases very rapidly with the energy in light elements.

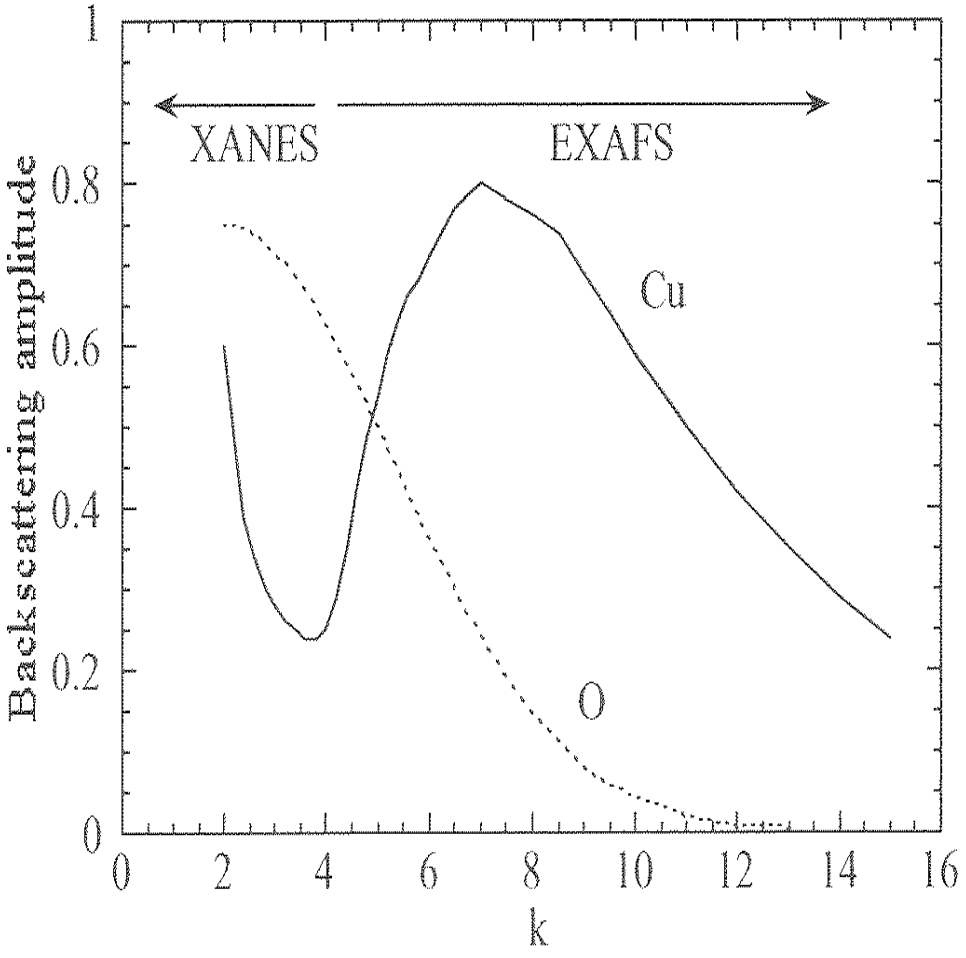

$$F_j(k) = \frac{1}{k}\sum_l (i)^{2l+1}(2l+1)\,e^{i\delta_l^j}\,\sin\delta_l^j$$

Biological example

Low temperature photolysis of myoglobin

$$\text{MbCO} \xrightarrow[T < 40K]{h\nu} \text{Mb*CO}$$

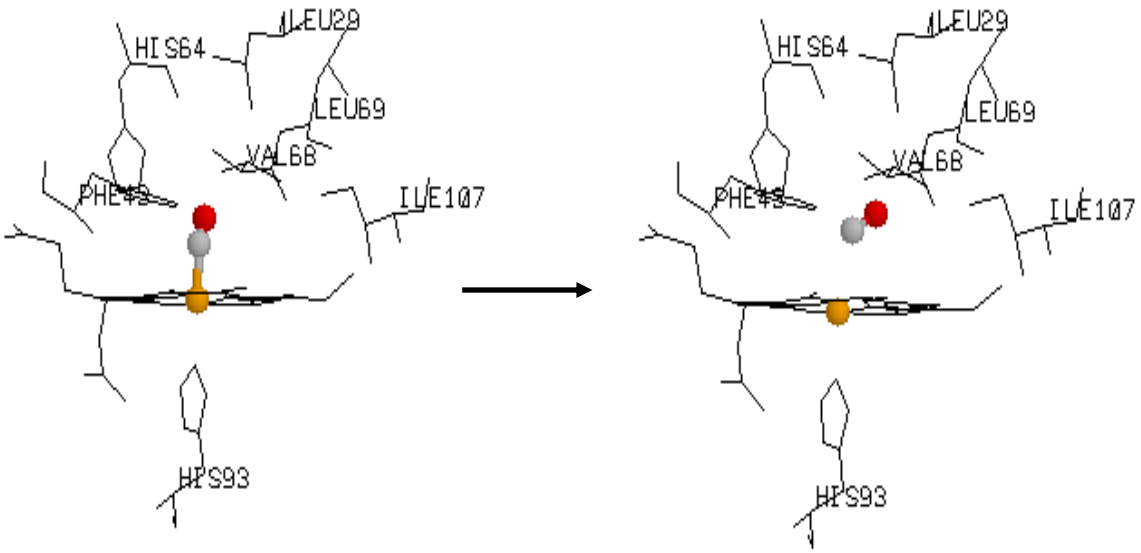

Exp. by S. Della Longa et al. J. Synch. Rad. (1999) **8**, 1138

myoglobin single crystal

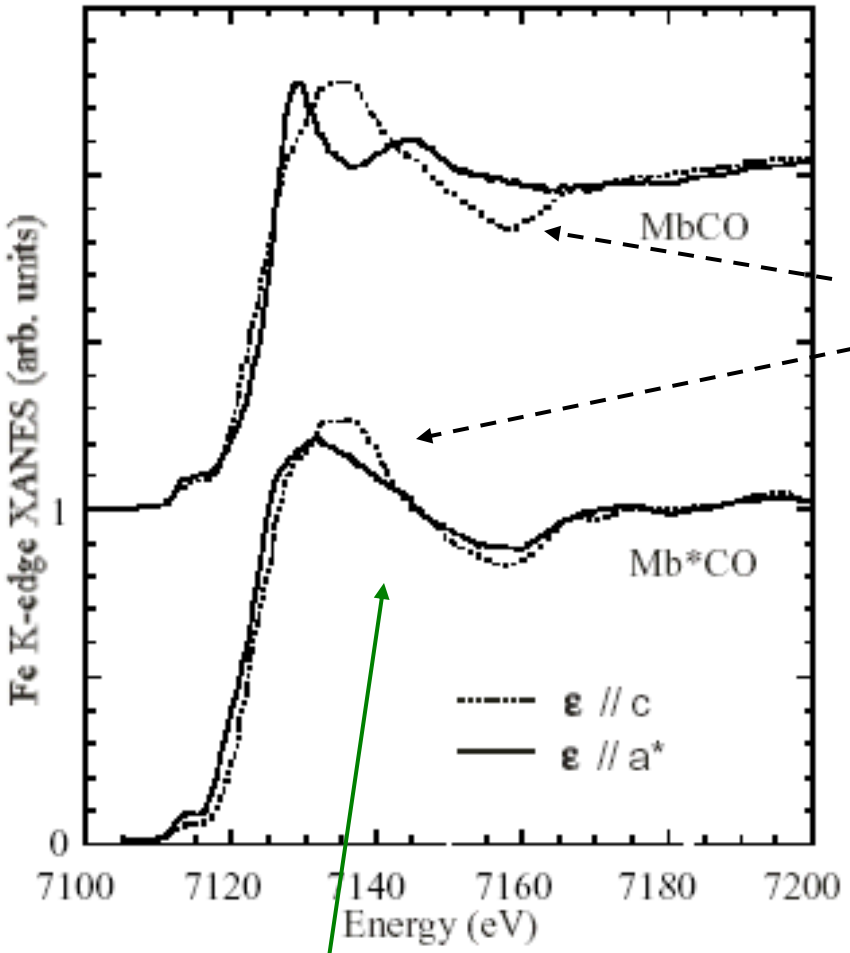

Heme plane

Most of the differences are in the energy range 0 – 80 eV

Two ways to calculate the scattering path operator

- by series:
- Exactly: all MS contributions are included

We have developed a new fitting method, called MXAN, that use the exact calculation of the scattering path operator

i) We work in the energy space
ii) We can start from the edge
iii) We can use polarization dependent spectra

To perform structural fits

- Initial geometrical configurations
- Exp. data

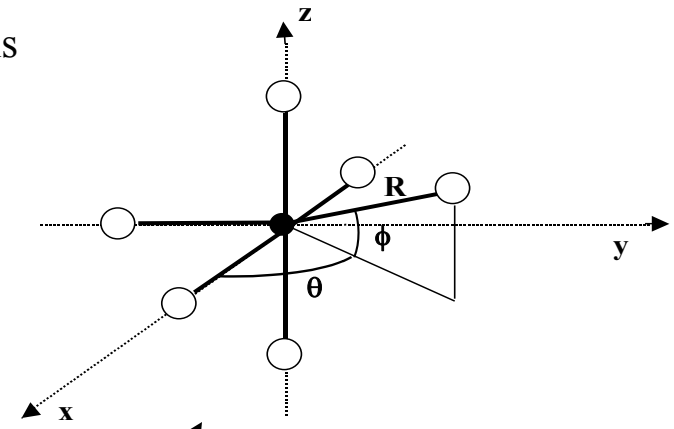

We generate hundred of theor.
spectra by moving atomic coordinates

The potential is calculated at each step – Norman criterion

Minimization of error function

$$R_{sq}^{\ 2} = \sum_{i=1}^{N} \{[y_i^{th.}(..r_n, \theta_n, ..) - y_i^{exp.}]^2 / \varepsilon_i^2\} w_i / \sum_{i=1}^{N} w_i$$

By comparison with exp. data we can fit relevant structural parameters

M. Benfatto and S. Della Longa J. Synch. Rad. **8**, 1087 (2001)
S. Della Longa et al. PRL **87**, 155501 (2001)
M. Benfatto et al. J. Synch. Rad. **10**, 51 (2003)

Transition metals in water solution

fits include Hydrogen atoms

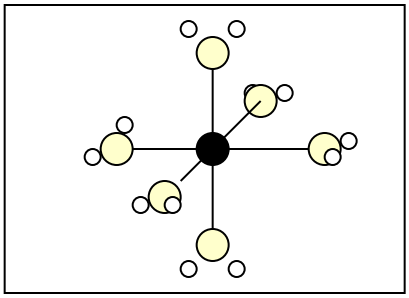

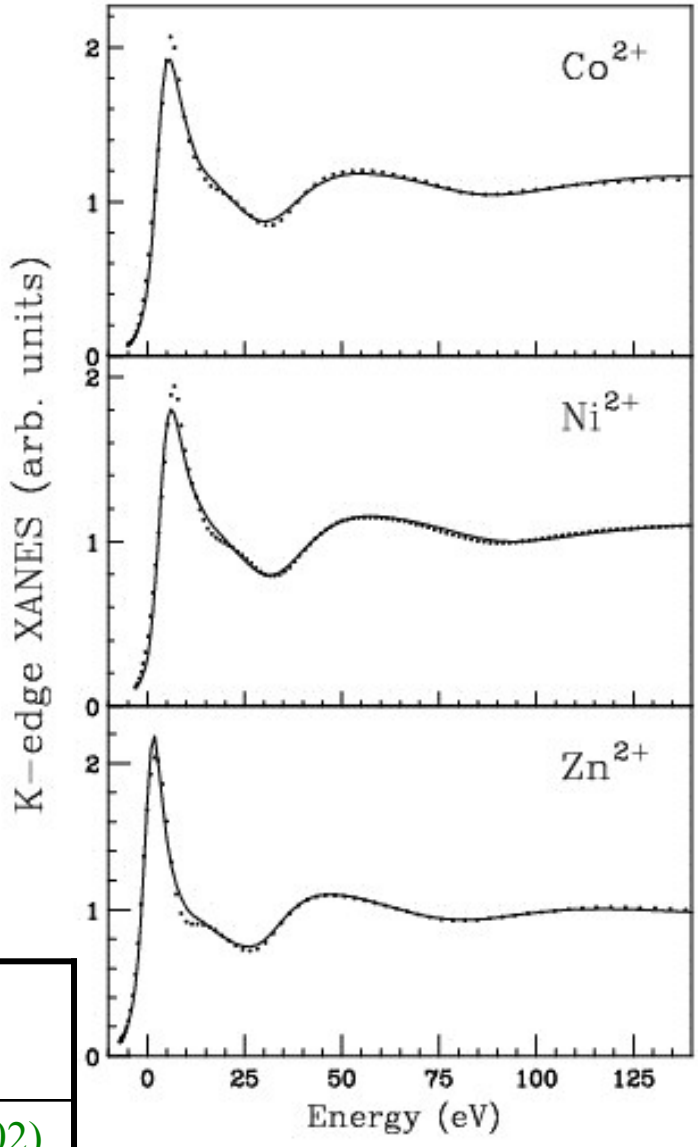

MXAN

GNXAS

	R(Å)	R(Å)
Co^{2+}	2.06(0.03)	2.092(0.002)
Ni^{2+}	2.04(0.03)	2.072(0.002)
Zn^{2+}	2.06(0.02)	2.078(0.002)

P. D'Angelo et al. (2002) Phys. Rev B **66**, 064209

$Fe(CN)_6$ in water

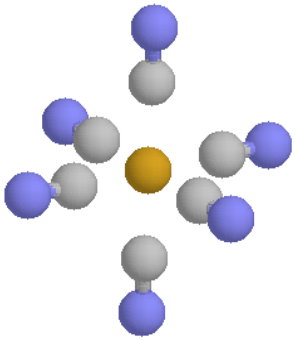

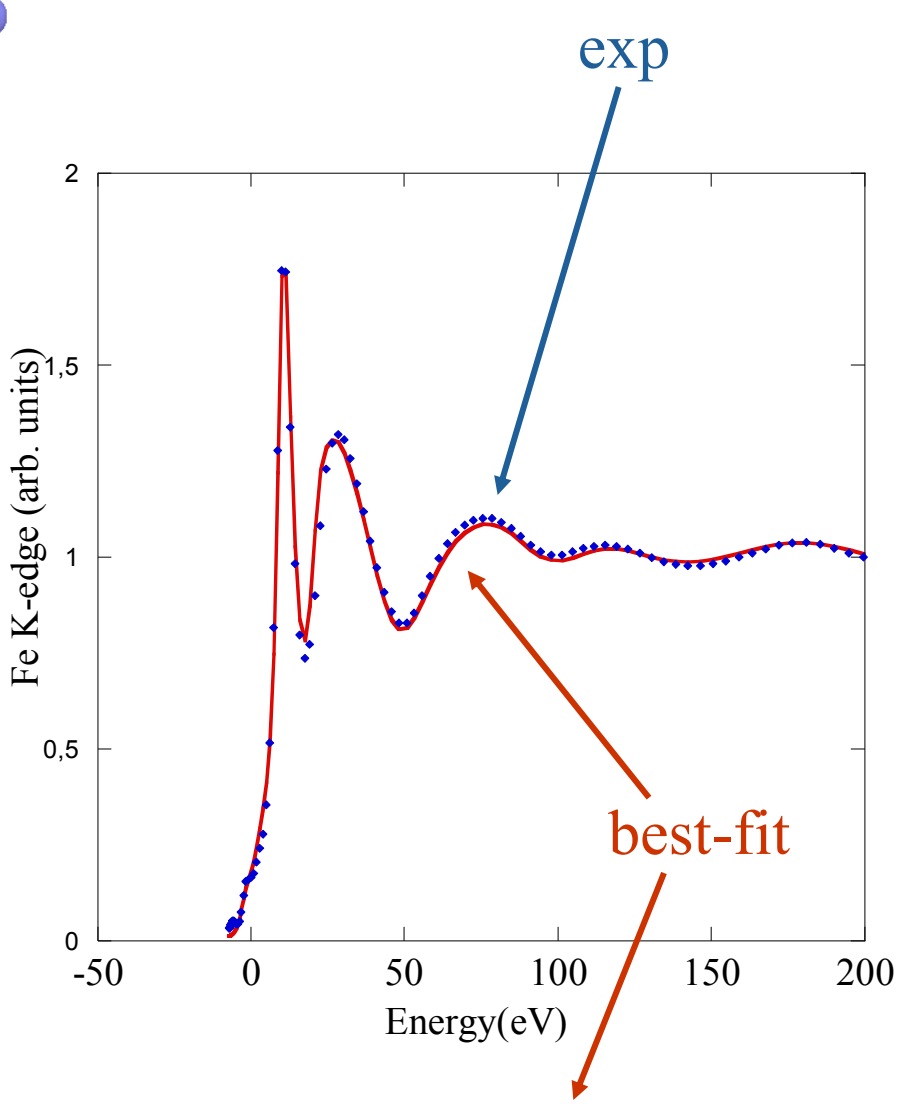

The best-fit condition corresponds to an octahedral symmetry with Fe-C distance of 1.92(0.01) Å and C-N distance of 1.21(0.01) Å

Previous GNXAS analysis (Westre et al. JACS 117 (1995)) reports Fe-C and Fe-N distances of 1.92 Å and 1.18 Å respectively

Test cases indicate a good structural reconstruction at the atomic resolution – 1-2 % although the muffin-tin approximation

high sensitivity to the structural changes very weak dependence to the no-structural parameters – in the new version of MXAN it is also possible to calculate the statistical correlation between structural and non structural parameters.

Several applications

From the coordination geometry of metal site in proteins to the time-depended spectra in the fs time domaine (data from LCLS facility).

S. Della Longa et al. Biophy. Jour. (2003) **85**, 549
P. Frank et al. Inorganic Chemistry (2005) **44**, 1922
C Monesi et al. PRB **72**, 174104 (2005)
R. Sarangi et al. Inorganic Chemistry (2005) **44**, 9652
P. D'Angelo et al. JACS (2006) **128**, 1853
.....
M. Bortolus et al. JACS (2010) **132**,18057
R. Sarangi et al. Journal of Chemical Physics (2012), 137, 2015103
.....
P. Frank et al. Journal of Chemical Physics (2015), 142, 084310
G. Chillemi et al. Journal of Physical Chemistry A (2016), 120, 3958
M. Antalek, et al. Journal of Chemical Physics (2016), 145, 044318.
H.T. Lemke et al. Nature Communication (2017), 8, 15342 doi:10.1038

Coordination geometry of Cu^{2+} in water solution: a quite long story

- Fourfold - Fivefold - Sixfold coordination?

- J.T. distortion?

Car – Parrinello molecular dynamics calculation
A. Pasquarello et al. Science (2001)

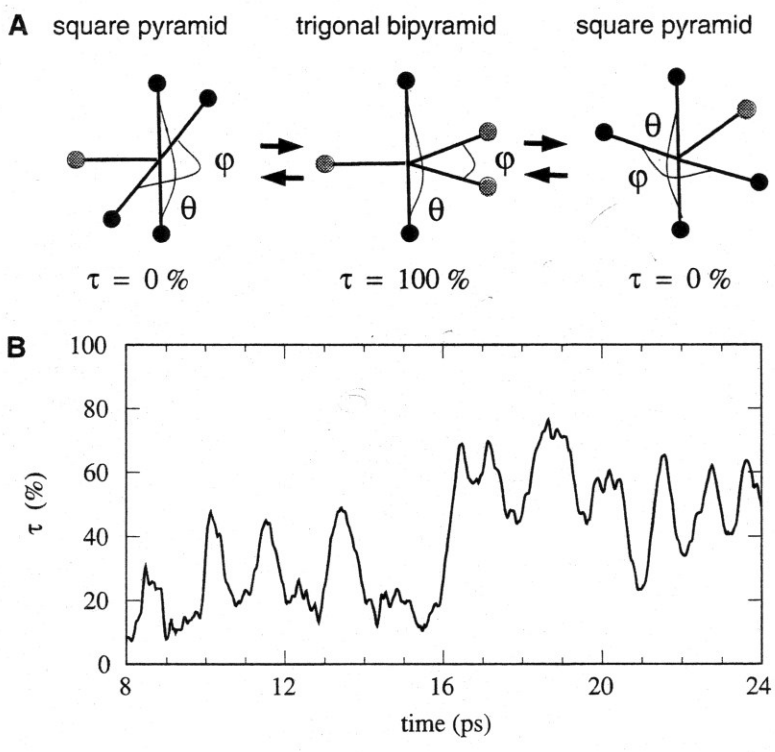

The first XAS analysis

0.1 M Cu^{2+} water solution
H atoms are included

GNXAS analysis

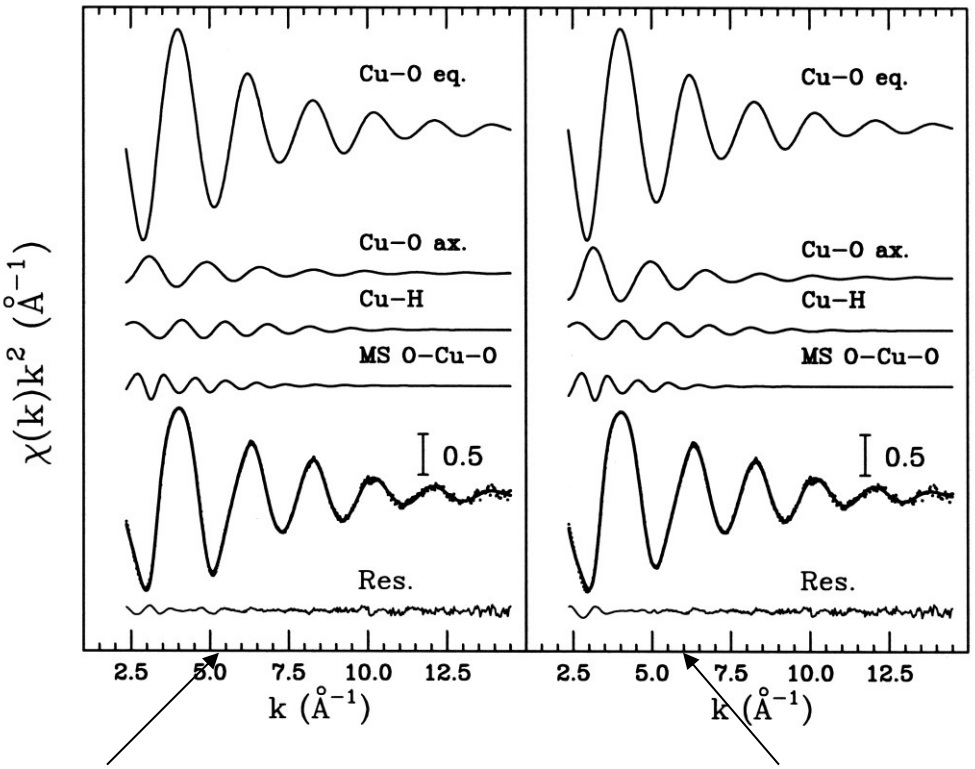

Fivefold coordination

sixfold coordination

Two geometries with the same accuracy

4 equa. O at 1.96 Angs
1 axial O at 2.36 Angs

4 equa. O at 1.96 Angs
2 axial O at 2.36 Angs

M. Benfatto et al. Phys. Rev B 65 (2002)

MXAN analysis

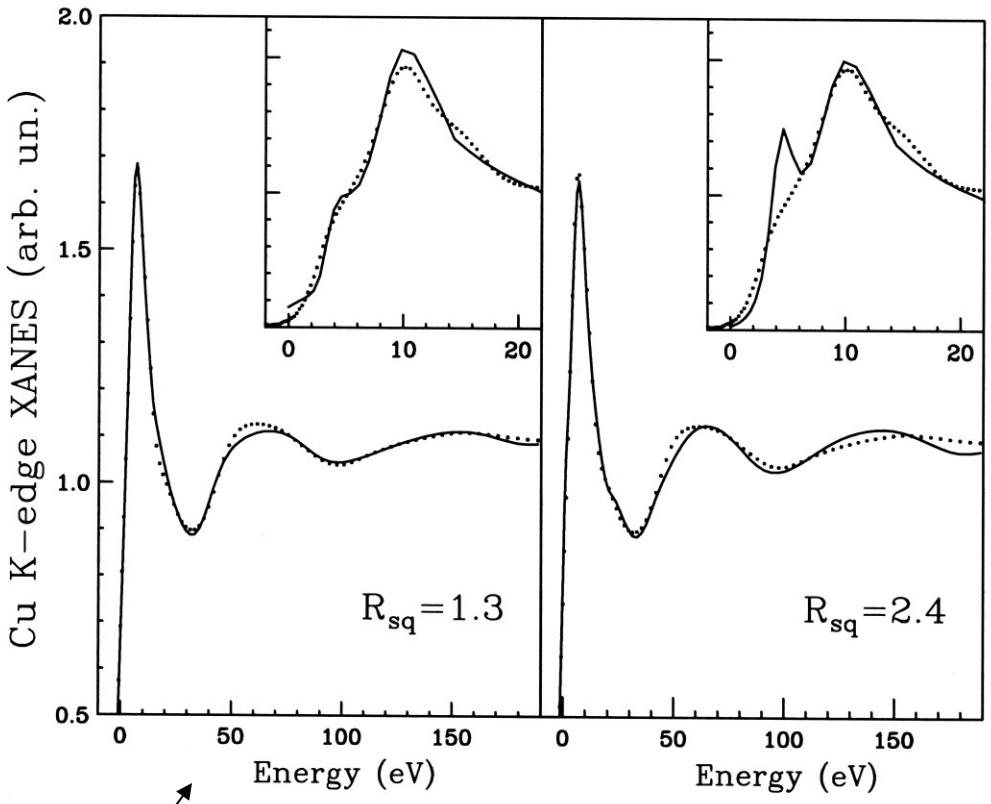

Fivefold coordination

sixfold coordination

Two different solutions

4 equa. O at 1.97(1) Angs
1 axial O at 2.39(6) Angs

4 equa. O at 1.99(1) Angs
2 axial O at 2.56(4) Angs

Combining the two possible solutions

An average fivefold coordination geometry

	N	R	σ^2
Cu-$O_{eq.}$	4	1.956(4)	0.0053(5)
Cu-$O_{ax.}$	1	2.36(2)	0.010(3)

The second XAS analysis: we also allow the movements of the four waters out from the average equatorial plane and more geometries

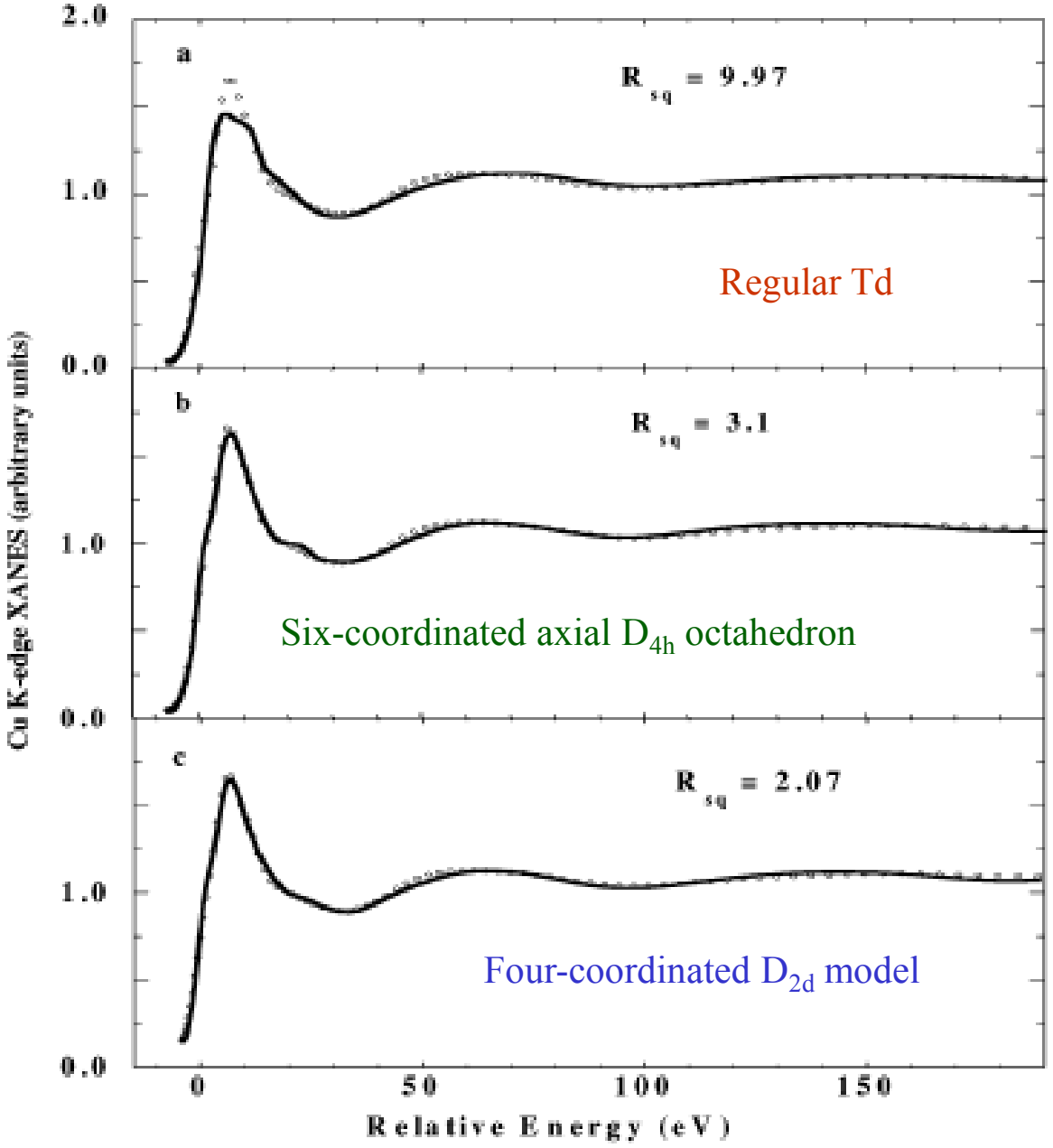

P. Frank et al. Inorganic Chemistry (2005)

Axial elongated square pyramidal model

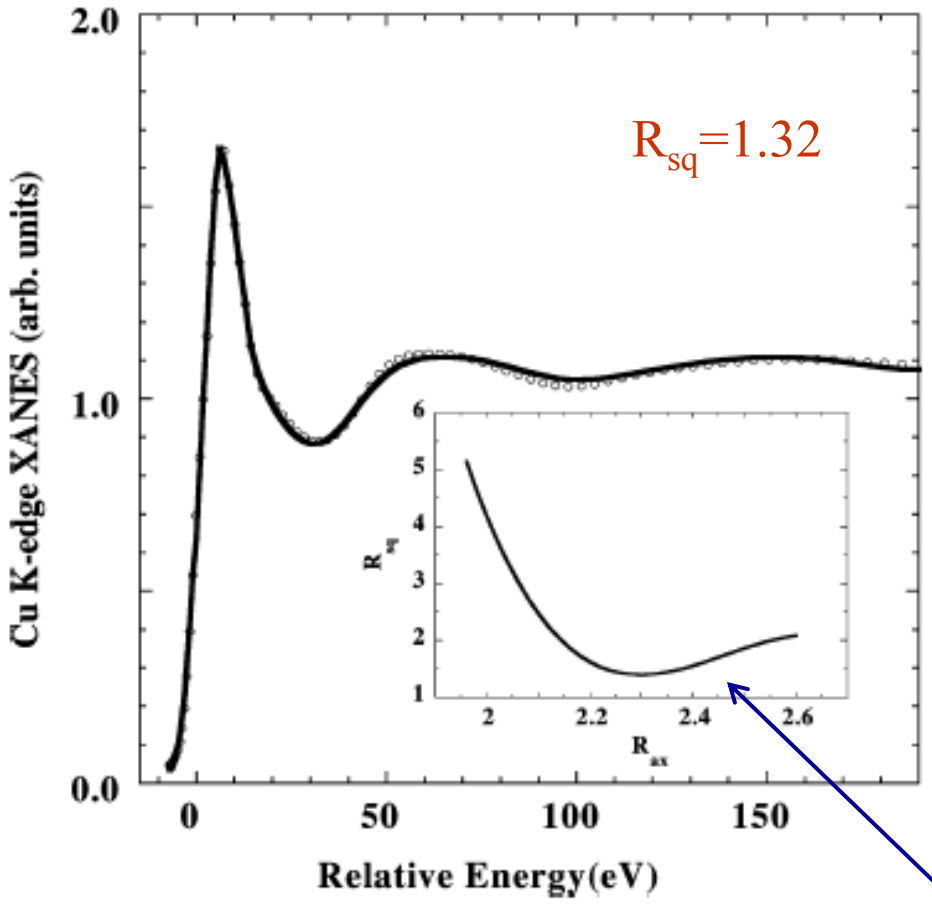

R_{sq} as function of Cu-O_{ax} distance

equatorial symmetry: D_{2d}[a]	R_{1eq} (Å)	R_{2eq} (Å)
four coordinate	1.96 ± 0.02	1.96 ± 0.02
five coordinate	1.98 ± 0.03	1.95 ± 0.03
six coordinate	1.99 ± 0.04	1.99 ± 0.04

R_{ax} (Å)	α (deg)	Γc (eV)[b]	R_{sq}
	13 ± 4.0	1.94	2.07
2.35 ± 0.05	17 ± 4	1.77	1.32
2.63 ± 0.05	7 ± 12	2.05	3.1

The third part of the story

Liquid and frozen (10 K) Cu solution

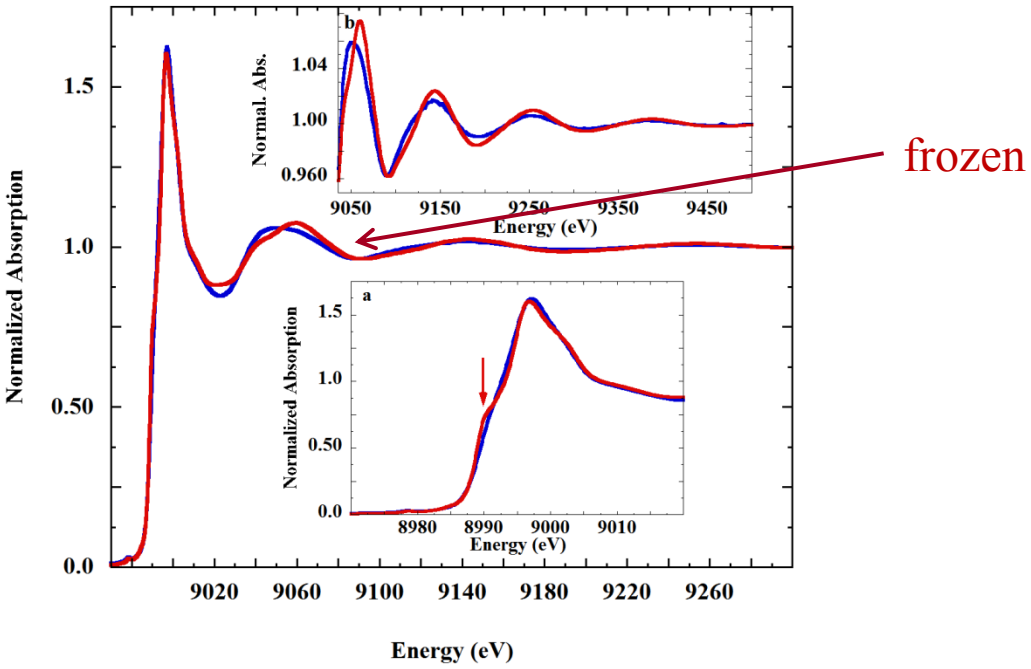

The frozen is not the liquid without smoothing

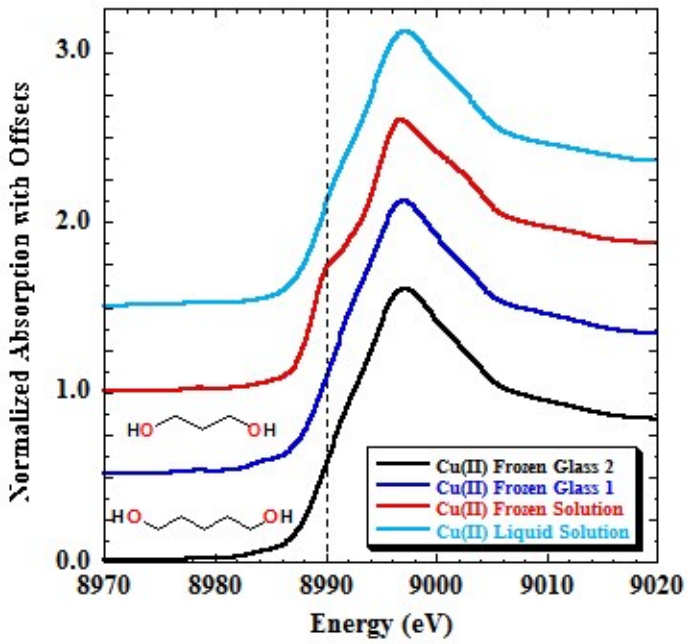

P. Frank, M. Benfatto et al. Jour. of Chem. Phys. 142, 084310 (2015)

MXAN analysis - Liquid water

4 equatorial + (1+1) splitted axials + 2sh of water

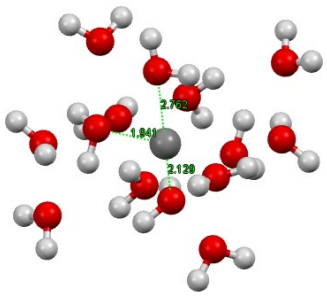

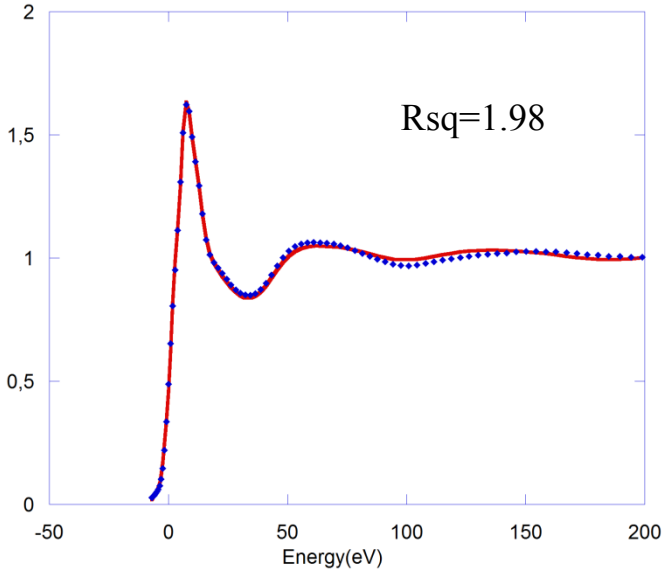

Oh JT distorted cluster + 2sh of water

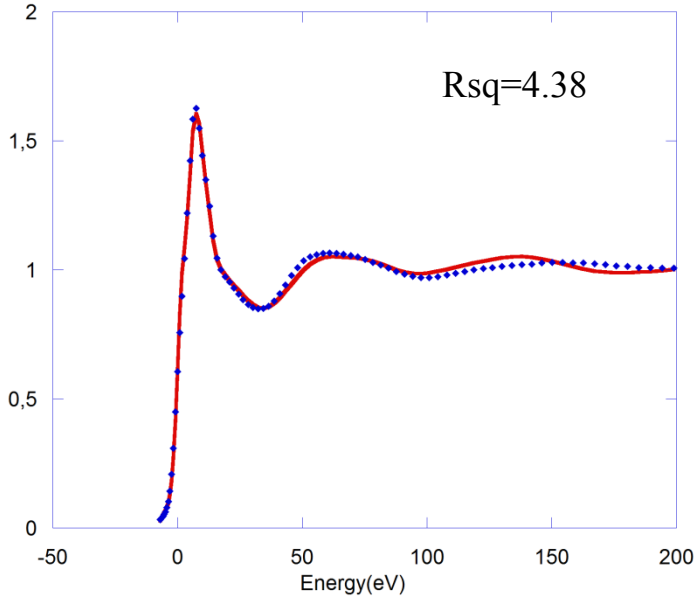

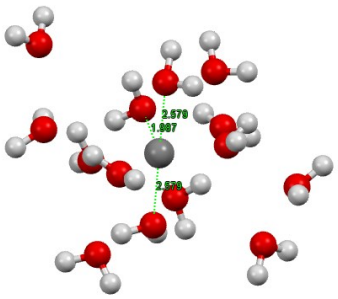

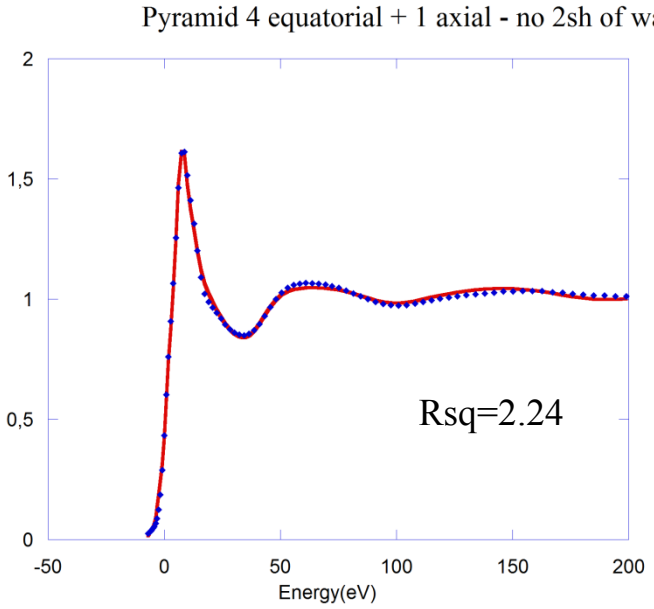

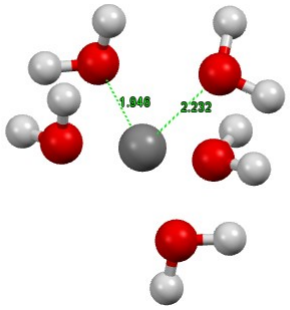

We have also tried other models but always with worst results

model	R_{eq}	R_{ax}	R_{ax}	R_{sq}
4eq. + (1+1) ax.	1.94±0.01	2.13±0.09	2.76±0.07	1.98
Oh JT Dist.	1.99±0.01	2.58±0.03	2.58±0.03	4.38
pyramid	1.95±0.03	2.26±0.02		2.24

Splitted axial and Oh-JT have a second shell of waters at about 3.8 Å

Compared with the previous results we have here the same equatorial findings and some slight differences in the axial determination – new version of MXAN and different H orientation

Liquid water with two sites

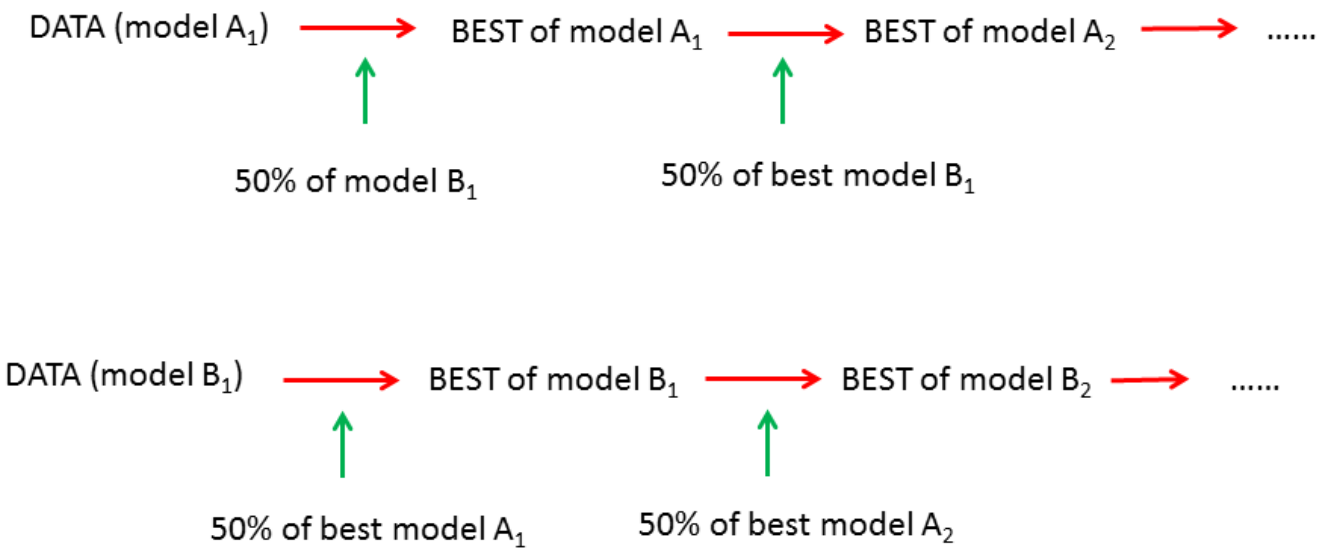

Model A : 4 equatorial + (1+1) splitted axials + 2sh of water

Model B : pyramid model

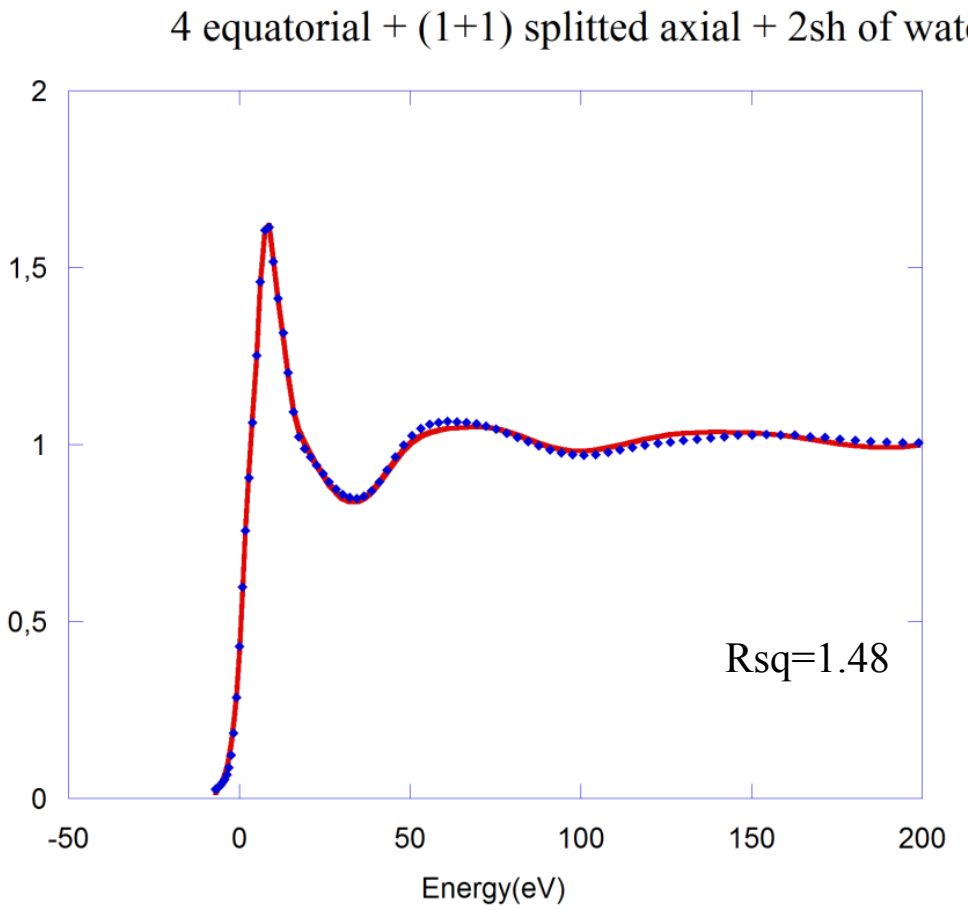

During the iterations R_{sq} goes down from about 2.0 to 1.5

model	R_{eq}	R_{ax}	R_{ax}	R_{sq}
4eq. + (1+1) ax.	1.94±0.02	2.06±0.07	2.99±0.22	1.49
pyramid	1.95±0.02	2.23±0.11		1.51

The equatorial geometry is quite stable in all samples – the same numbers whatever the way to fit the data

The numbers of the axial part depends of the details of the fit although some geometries (Oh-JT , Td) produce much worse results

the two sites fit give better result – the system could be dimorphic

DFT study (P. Frank et al. IC (2005)) indicates an electrostatic interaction in the axial direction

To describe the axial geometry there is the need of many geometrical configurations that in liquid water can be thought as a real dynamical situation – we did MD simulation to test in details this idea

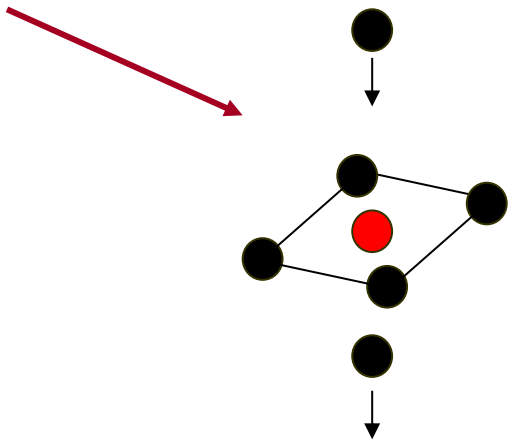

XAS and Molecular Dynamics

We use MD to generate thousands of geometrical configurations – each snapshot with a time step of 50 fs is used to generated one XANES spectrum – average using ~ 10^4 geometrical configuration

$$R_f(N) = \left[\sum_i [\sigma^N(E_i) - \sigma^{N-1}(E_i)]^2 \right]^{1/2}$$

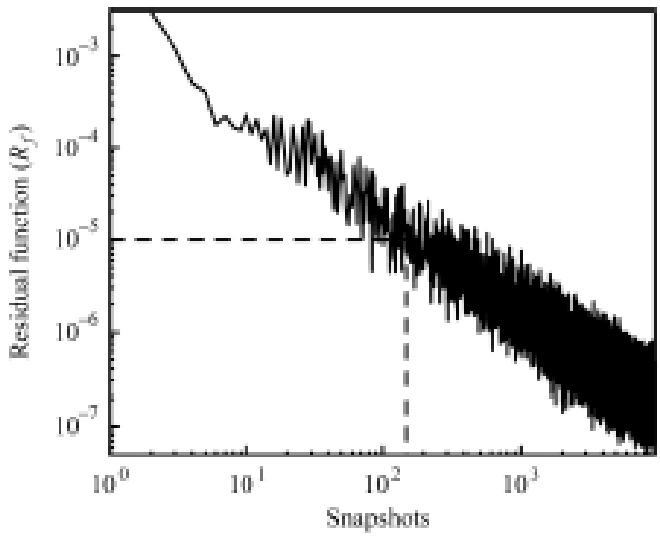

MD details

- Classical MD – solve the Newton's equations of motion for a given Force field
- Two body potential formed by two parts: bonded and nobonded interactions (LJ and Electrostatic interactions) – if needed corrections to account QM effects
- GROMACS
- Time steps of 2 fs
- Before to extract the trajectories the system is thermal equilibrated for several ps by using a thermal bath at a given temperature

More details

$$\mathbf{f}_i = m_i \cdot \mathbf{a}_i \qquad \mathbf{f}_i = -\frac{\delta V}{\delta \mathbf{r}_i}$$

$$V(\mathbf{r}_1, \mathbf{r}_2, ..., \mathbf{r}_n) = \sum_{bond} \frac{1}{2} k_{b_0} \left(b_n - b_{0_n}\right)^2 + \sum_{angle} \frac{1}{2} k_{\theta_0} \left(\theta_n - \theta_{0_n}\right)^2 +$$

$$+ \sum_{\substack{improper \\ dihedral}} \frac{1}{2} k_{\xi_0} \left(\xi_n - \xi_{0_n}\right)^2 + \sum_{dihedral} 1 + \cos\left(m_n \phi_n - \delta_n\right)^2 +$$

$$+ \sum_{\substack{nonbonded \\ pairs(ij)}} \left(\left(\frac{C_{ij}^{(12)}}{r_{ij}^{12}} - \frac{C_{ij}^{(6)}}{r_{ij}^{6}} \right) + \frac{1}{4\pi\varepsilon_0} \frac{q_i q_j}{\varepsilon_r r_{ij}} \right)$$

L-J potential ⟶ van der Waals interactions. $C^{(6)}$ is the constant in the term describing the dispersion attractive force between atoms; $C^{(12)}$ is in the term that describes interatomic electron cloud repulsion

Ni^{2+} in water – Ni Kedge

The case of typical two-body effective potential developed for Zn(II), Ni(II) and Co(II) in water

$$V = \frac{q_M q_O}{\varepsilon_r r_{MO}} + \frac{A_O}{r_{MO}^4} + \frac{B_O}{r_{MO}^6} + \frac{C_O}{r_{MO}^8} + \frac{D_O}{r_{MO}^{12}} + E_O e^{\frac{-r_O}{r_{MO}}} + \sum_{MH=MH1,MH2} \frac{q_M q_H}{\varepsilon_r r_{MH}} + \frac{A_H}{r_{MH}^4} + \frac{B_H}{r_{MH}^6} + \frac{C_H}{r_{MH}^8} + \frac{D_H}{r_{MH}^{12}}$$

There is a table for each of above parameters, H is hydrogen and O is oxygen

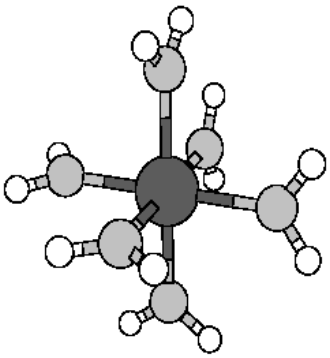

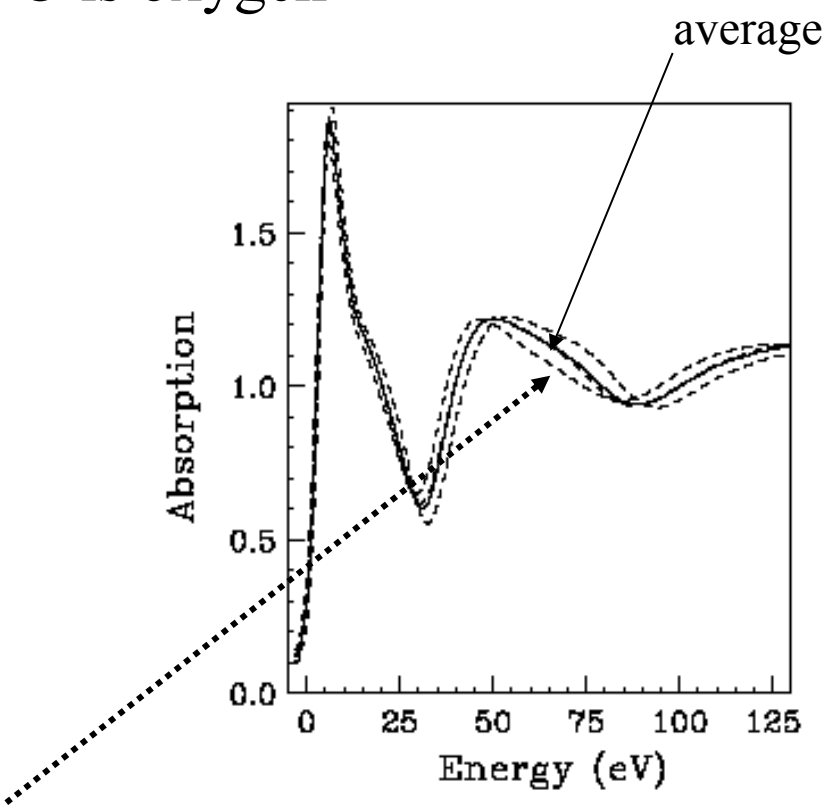

Calculations for some particular snapshots

Comparison between the averaged theoretical spectrum and a single theoretical spectrum at the symmetrical first shell configuration

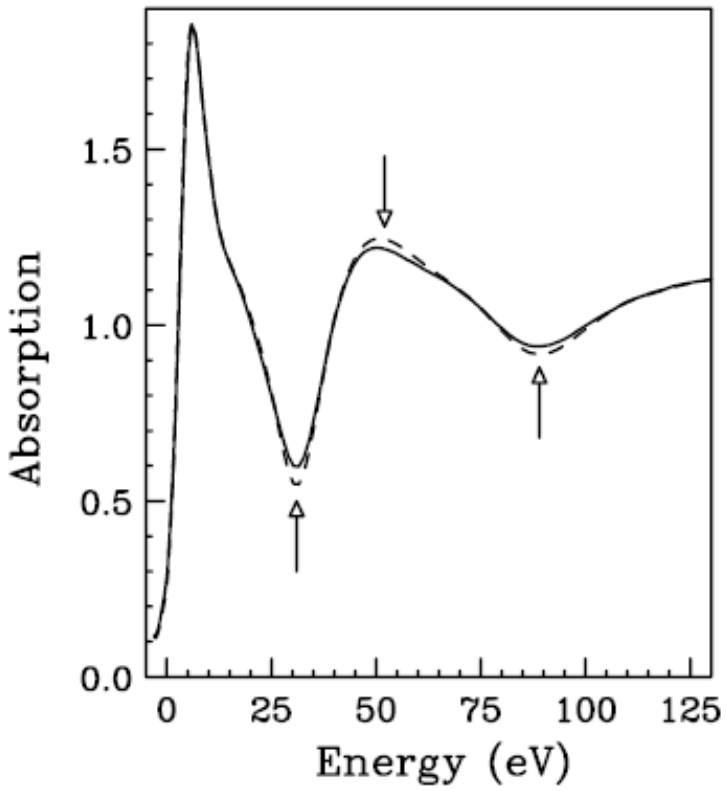

Arrows indicate the damping - very weak effect

including the second shell

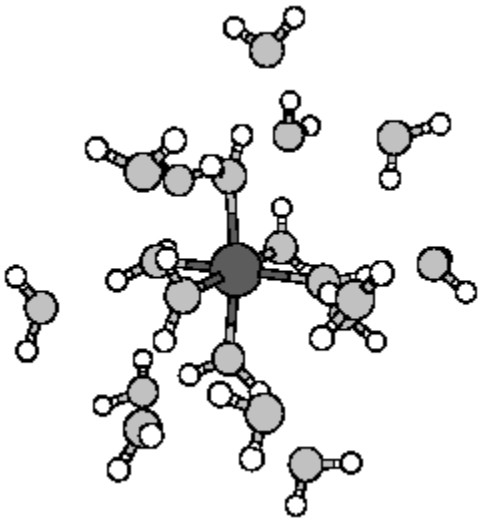

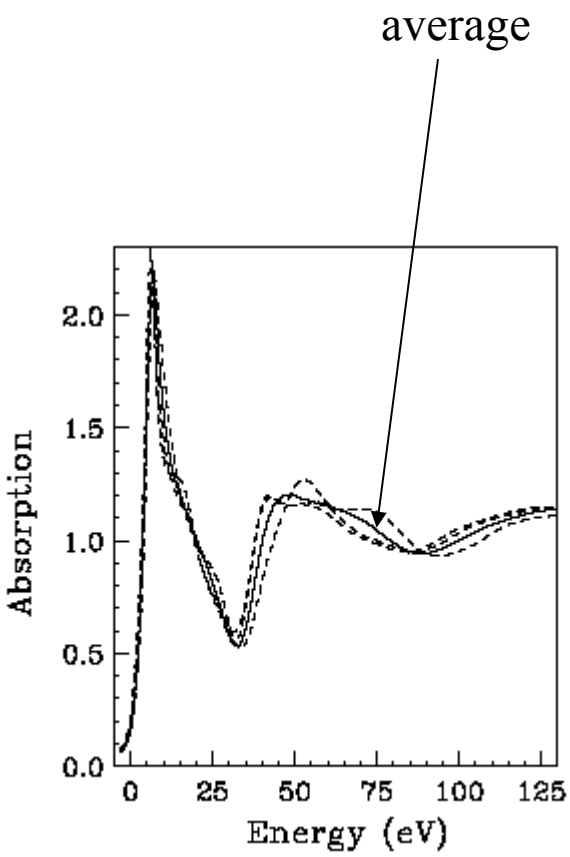

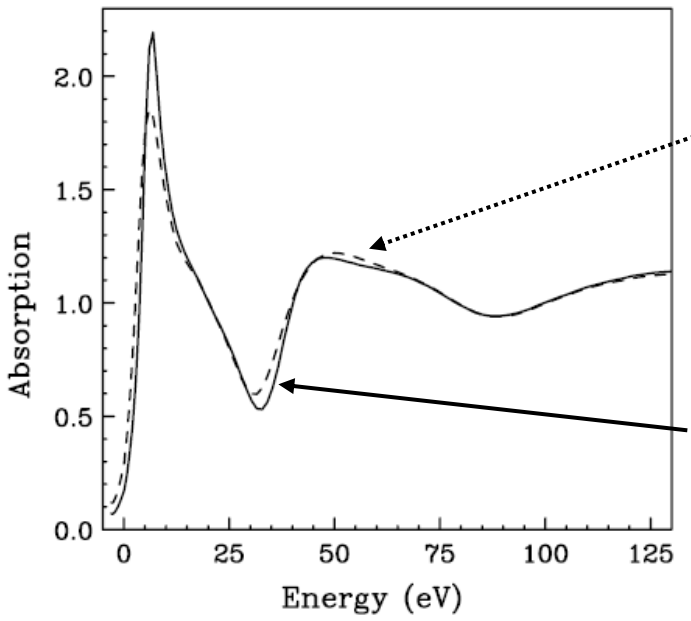

first shell average

first + second shells average

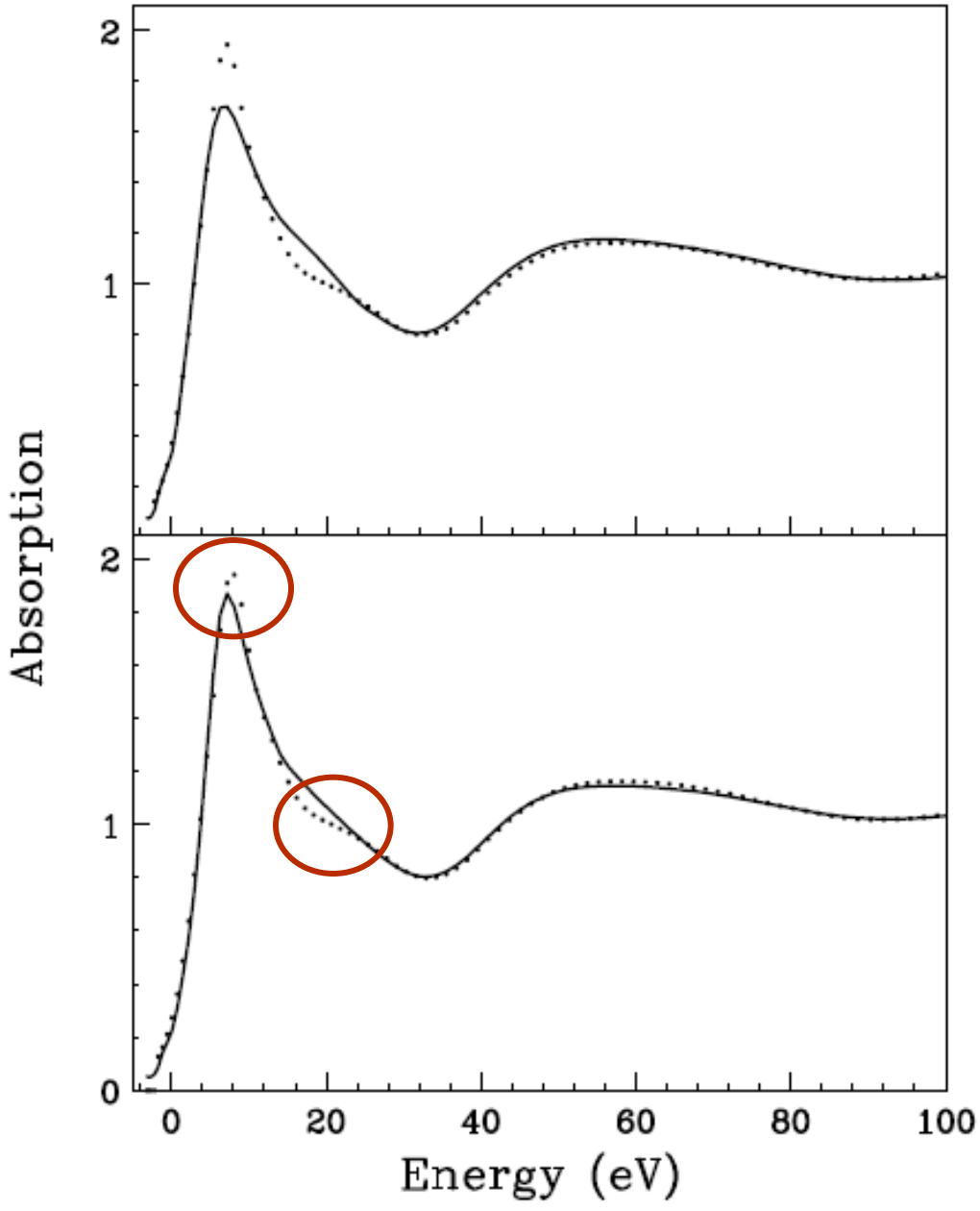

one shell fit

two shells fit

sizeable effects in the energy range 0 - 30 eV

The last part? of the story – MD of Cu in water

It is quite difficult to make MD simulation for this system because of

- the force-field parameters for classical MD
- exchange-correlation functional in the first-principle MD

The literature is full of different result: five-fold or six-fold hydratation structures.

All studies agree on the presence of stable four equatorial waters at about 1.94 – 1.96 Å

we performed MD imposing the equatorial geometry – The equatorial waters are like a single block and the $Cu(H_2O)_4^{2+}$ complex is immersed in 1098 water molecules.

we have looked to the axial dynamic for 10 ns

The cluster used in MXAN includes waters up to 4.5 Å, i.e. beyond the second hydratation shell

G. Chillemi, E. Pace, M.D'Abramo and M. Benfatto, (2016) Journal of Physical Chemistry 120, 3958.

two water models: SPC/E and TIP5P

SPC/E: charges on oxygen and H atoms
TIP5P: charges on H atoms and oxygen ion pairs

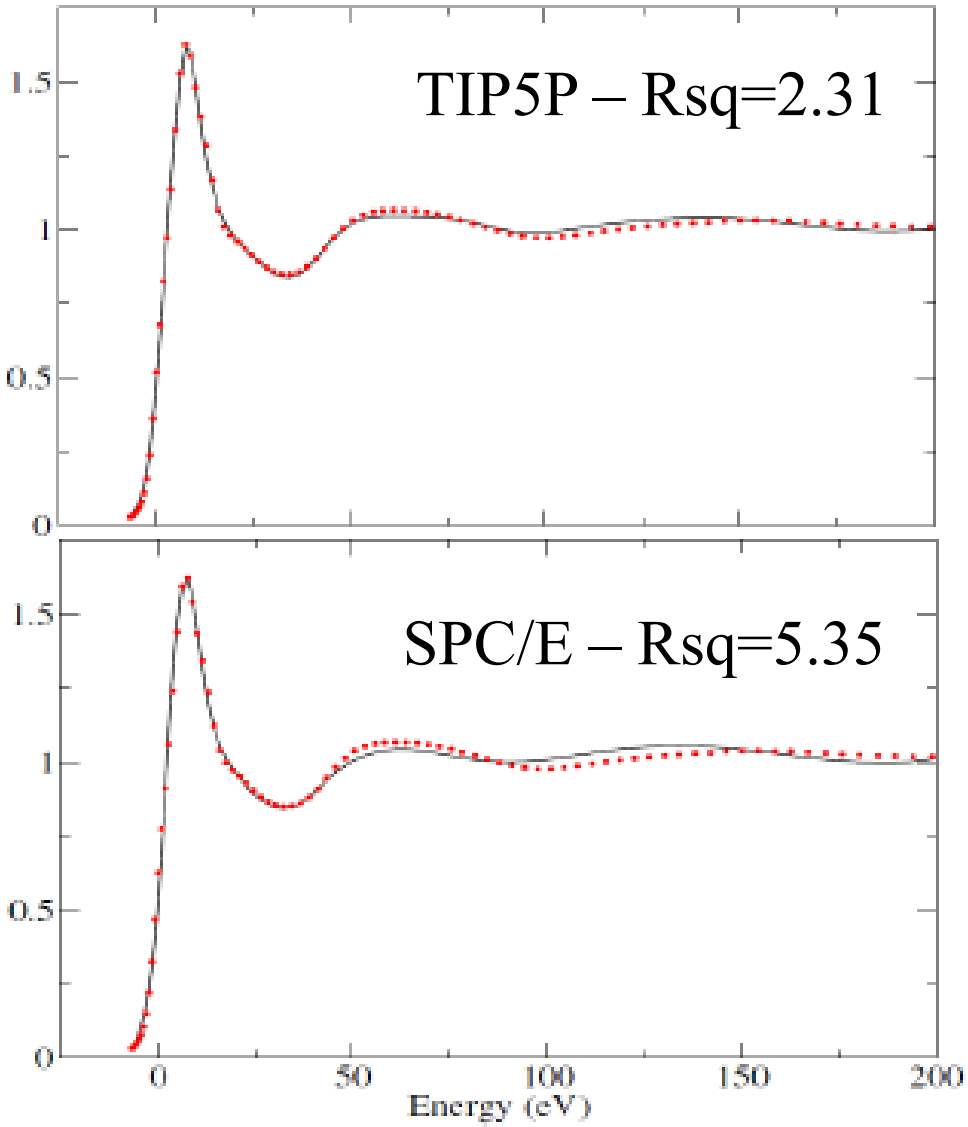

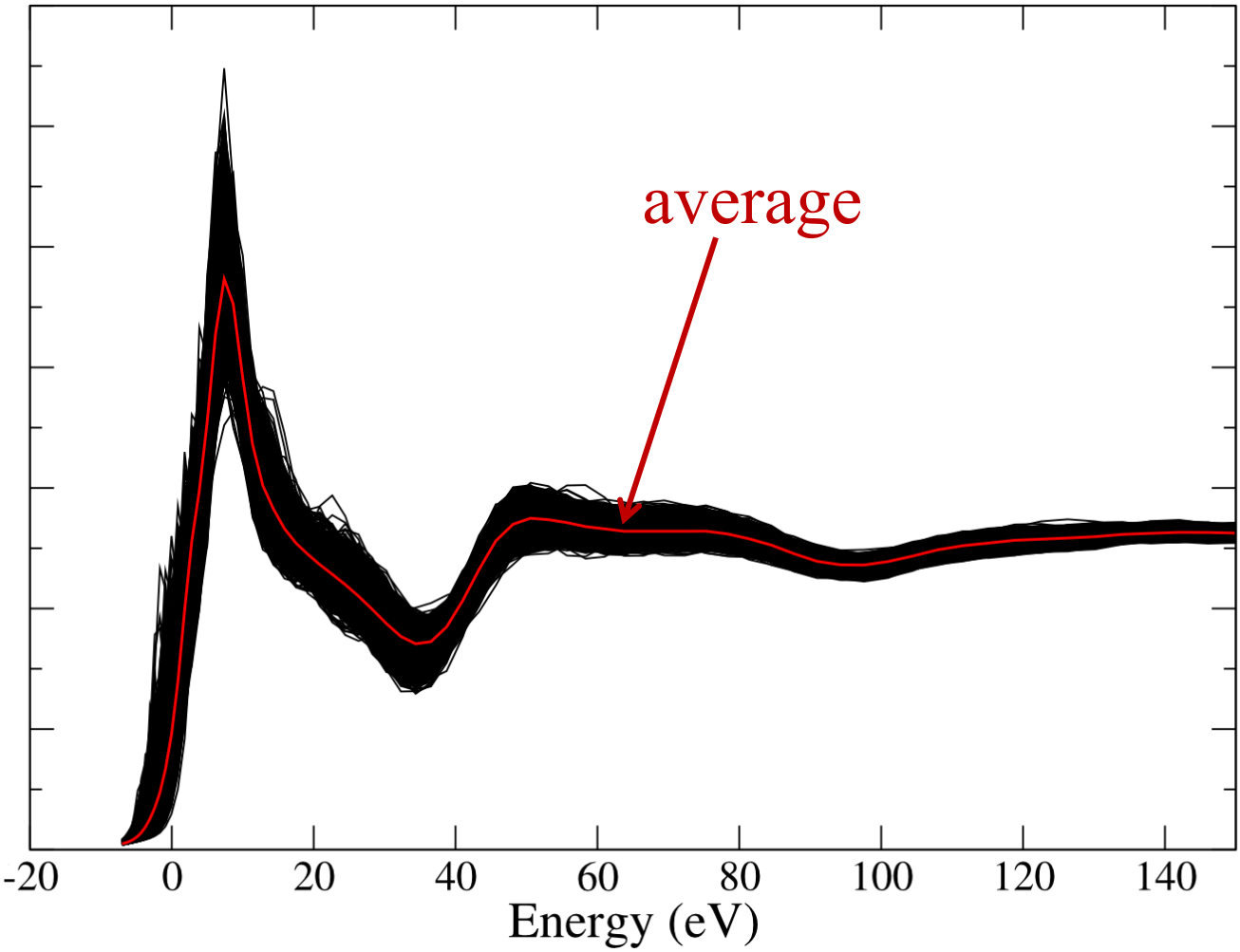

Comparison between the averaged theoretical XANES spectrum (without any damping) obtained using the TIP5P water model and several spectra associated with individual MD configurations (black lines)

static characterization

TIP5P

SPC/E

water by water

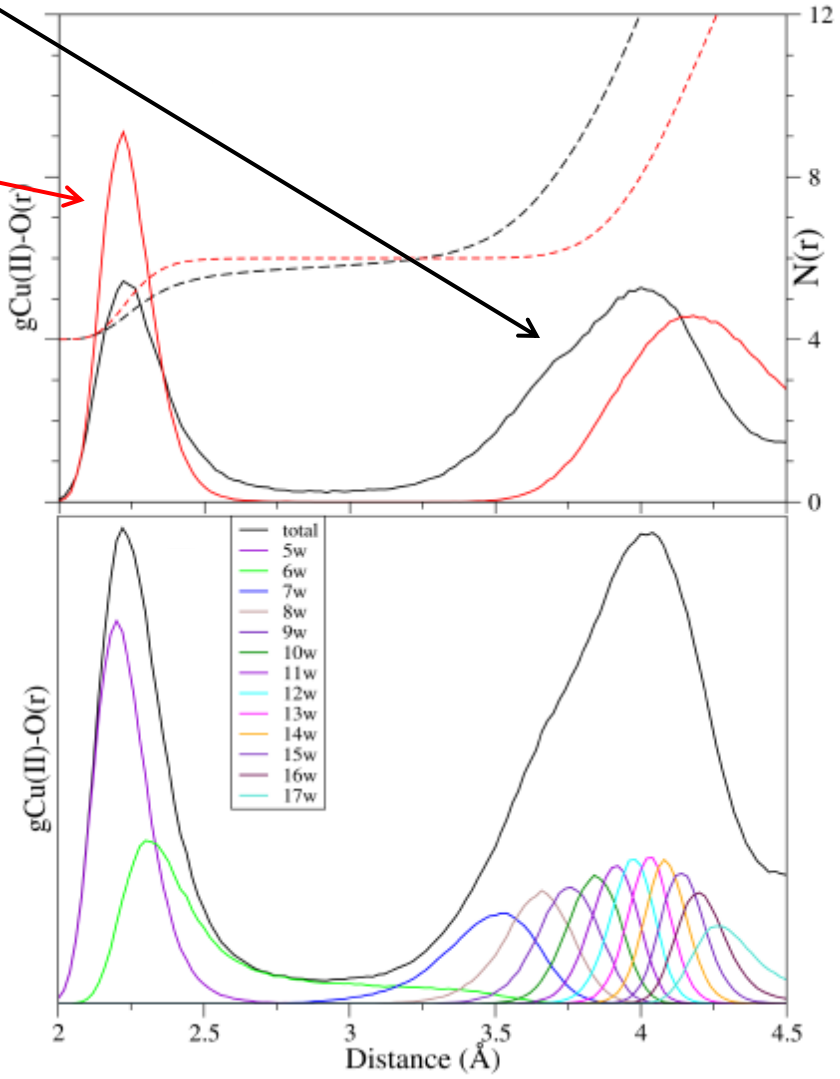

5th	6th
2.24±0.11	2.61±0.38

← Average distance for TIP5P model

Static XAS →

5th	6th
2.14±0.13	2.99±0.22

dynamical characterization

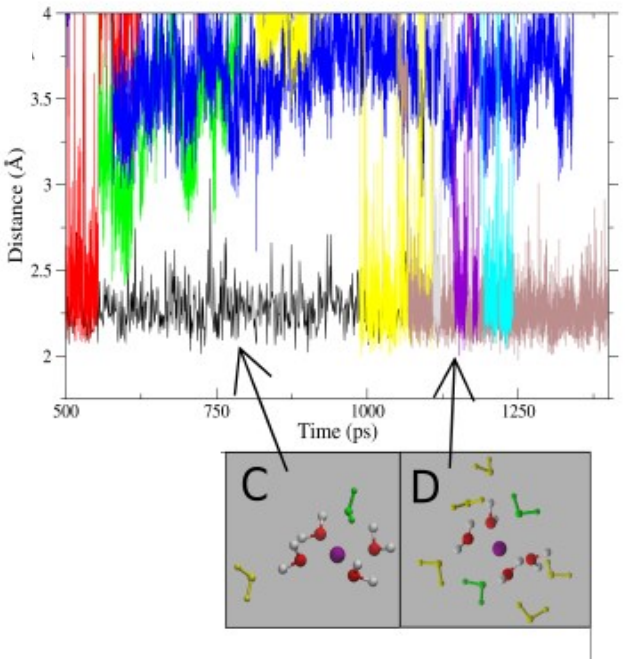

Cu-O distances as function of time – different colors for individual water – the hexa-hydrated structure is present for 54.9% of time while the penta-hydrated is for 43.2%

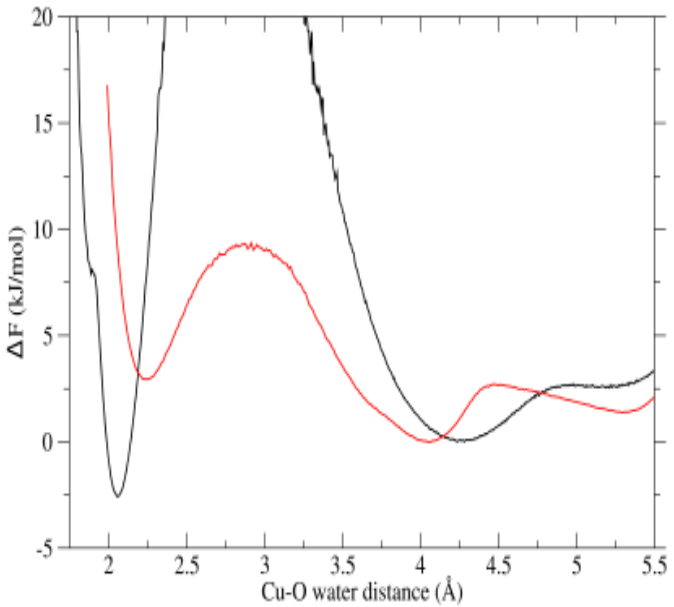

Free eenergy profile along the ion – water distance

the “strange case ” of Cl

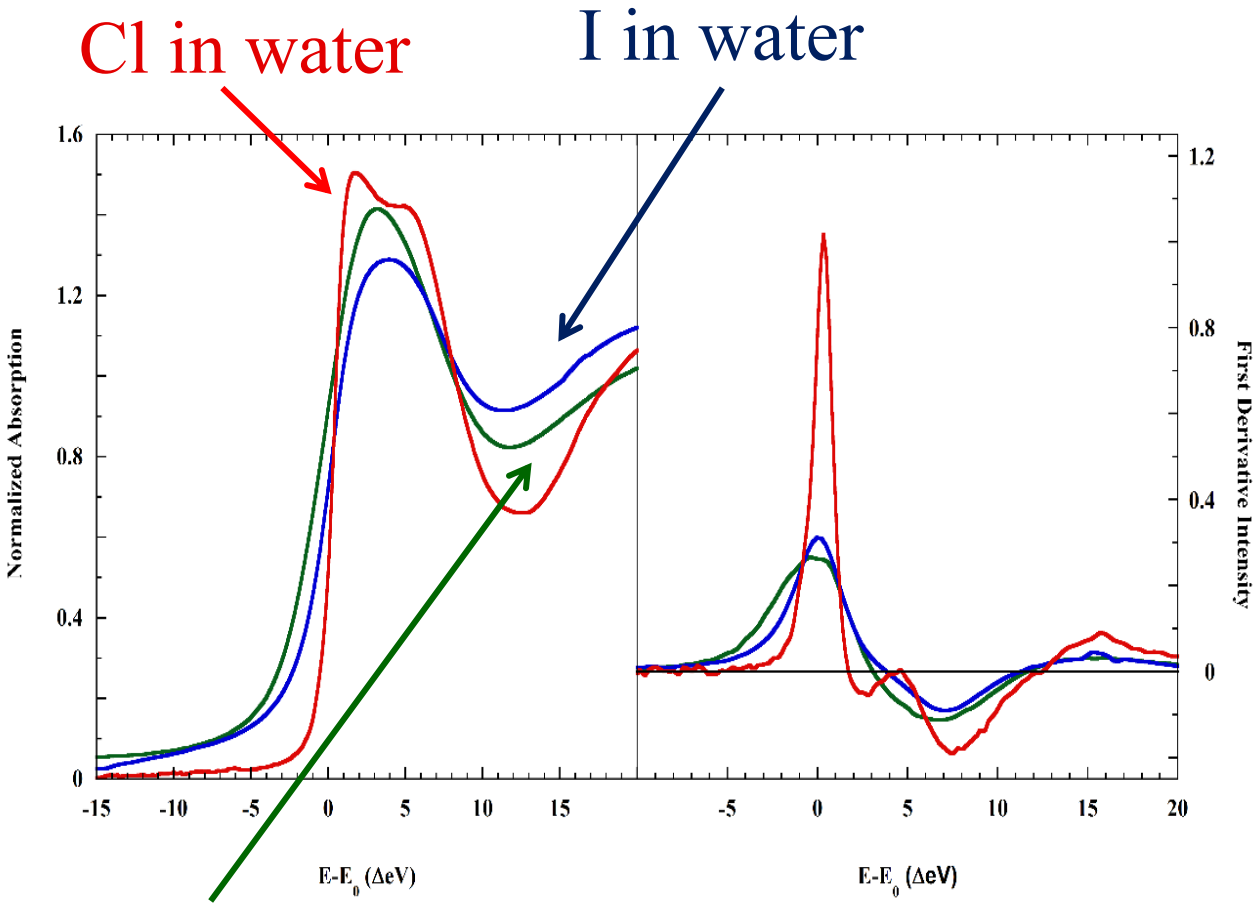

The three halide ions are all filled shell and iso-electronic ($3p^6$, $4p^6$, $5p^6$) – same ground state electronic configuration

M. Antalek, E. Pace, B. Hedman, K. Hodgson et al. (2016) The Journal of Chemical Physics 145 (4), 044318.

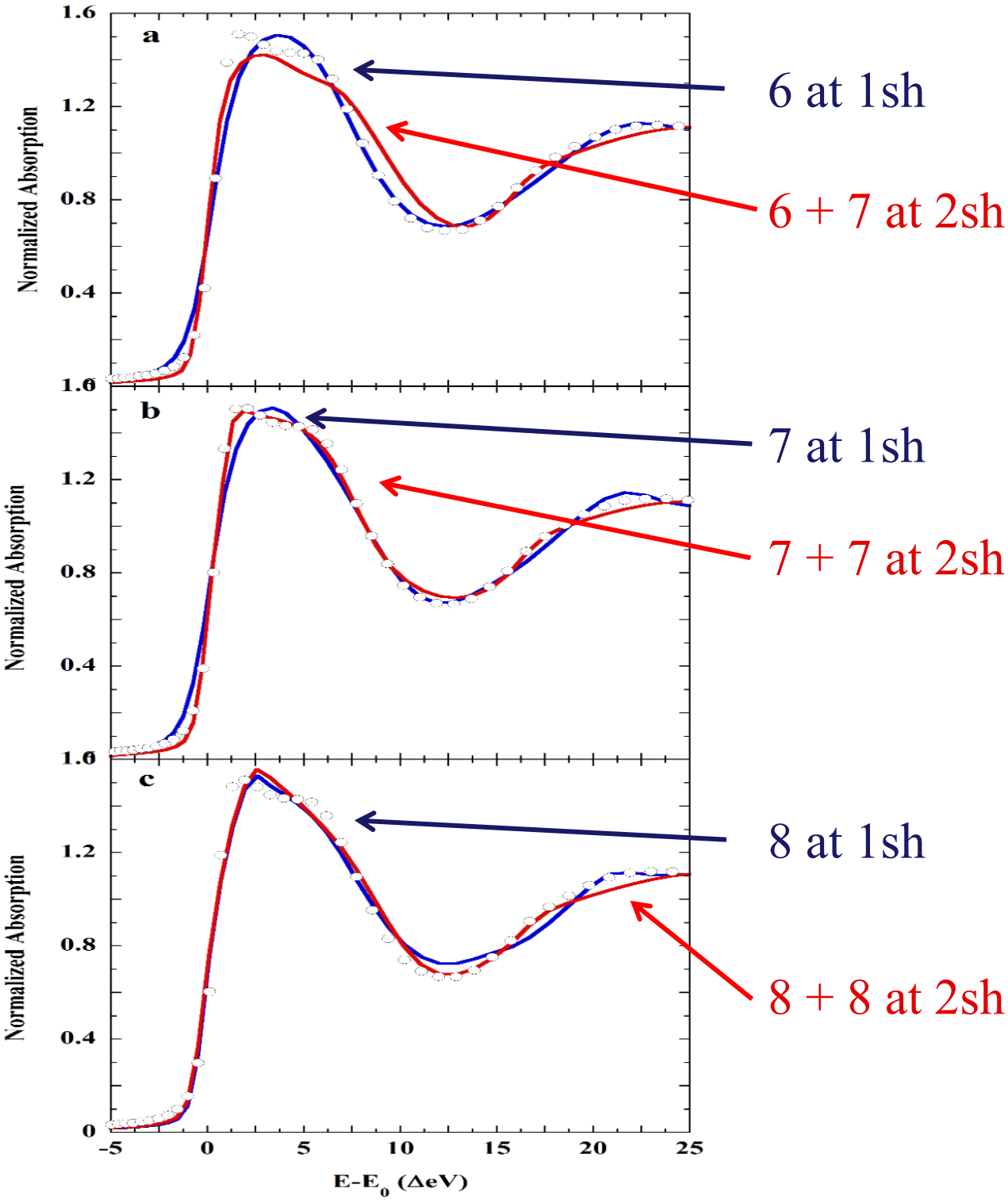

White points are the exp. data

Further refinement of the second shell

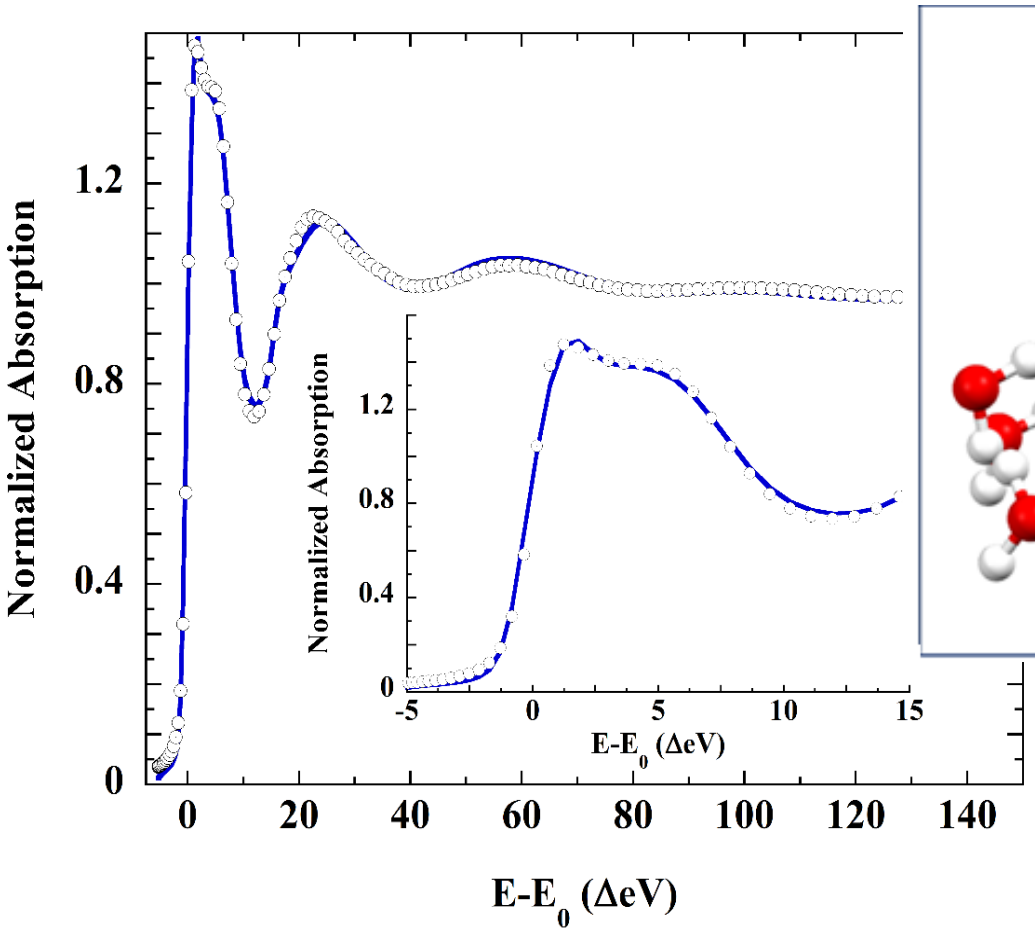

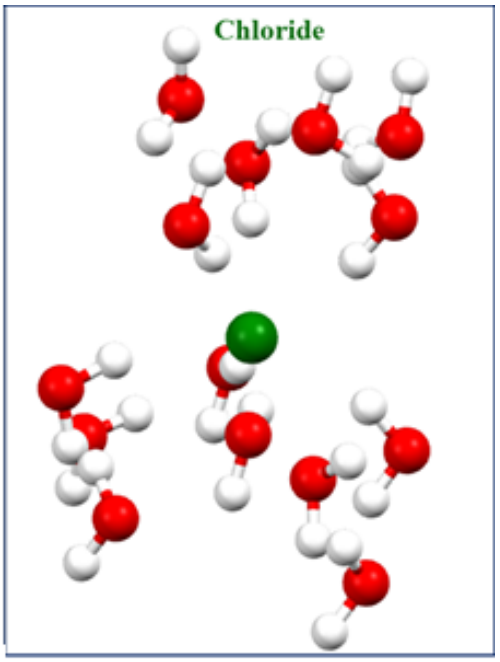

Shell	Cl-O (Å)[a,b]	Cl-H_{near} (Å)[a]	Cl-H_{far} (Å)[a]
7 waters	3.15±0.10	2.18±0.10	3.50±0.10
7 waters	4.14±0.31	3.76±0.38	4.89±0.30
		Prior Work	
CN[d]	Cl-O (Å)	Cl-H_{near} (Å)	Method[e]
6±1	3.1	2.2	ND,XRD
6.4±0.3	3.1±0.01	2.28±0.03	ND
6.4	3.3	2.28	AXD
---	3.14±0.02	---	SAXS
6.4	3.14±0.02	2.23±0.04	EXAFS

DM of Cl in water - three different L-J parameters L_E, M_E, and H_E for the SPC/E water model by Reif and Hünenberger – only $C^{(12)}$ changes

$$\left(\frac{C_{ij}^{(12)}}{r_{ij}^{12}} - \frac{C_{ij}^{(6)}}{r_{ij}^{6}} \right)$$

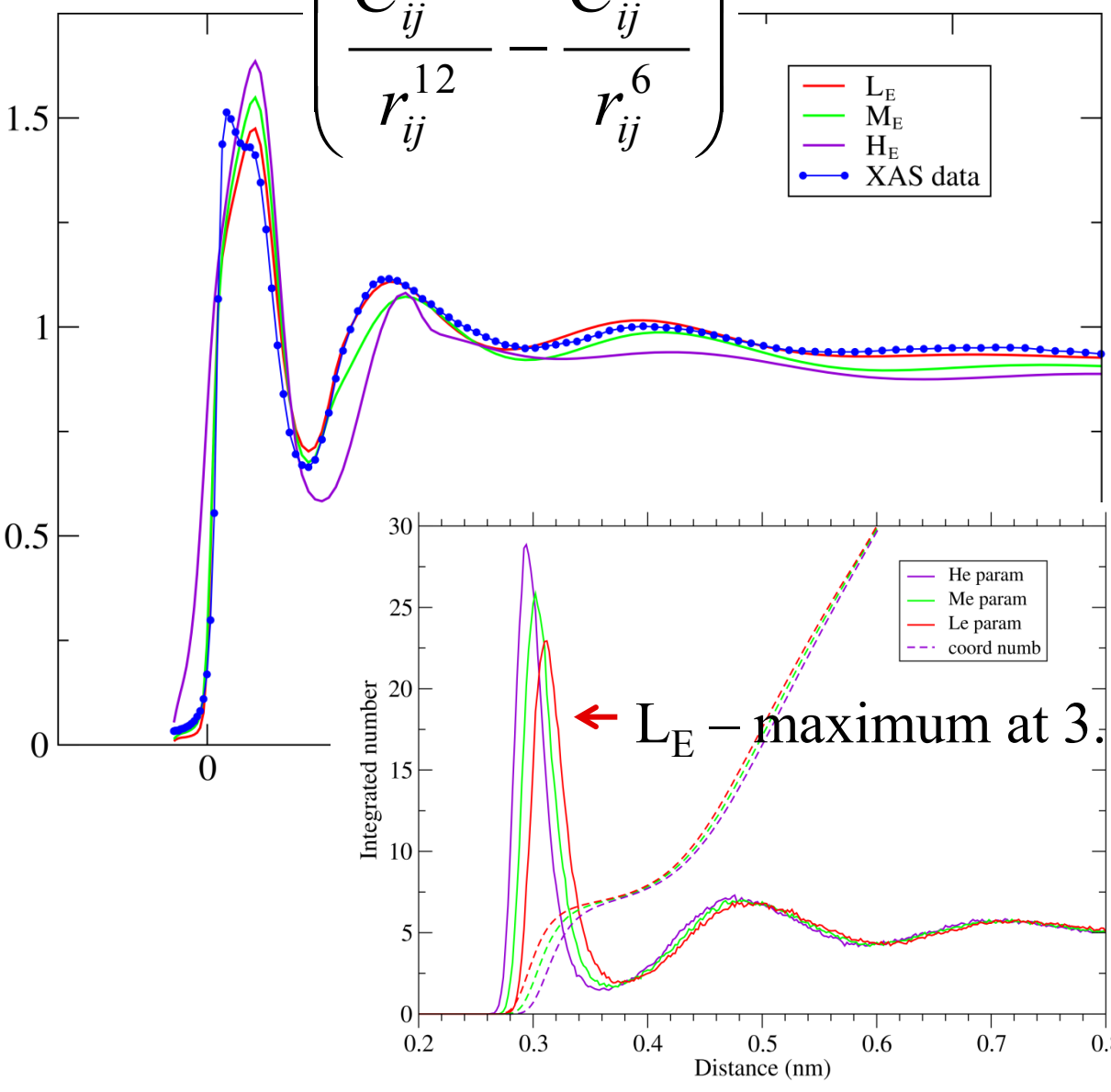

L_E – maximum at 3.11 Å

M. M. Reif, and P. H. Hünenberger,
J. Chem. Phys. **134** 144104 (2011).

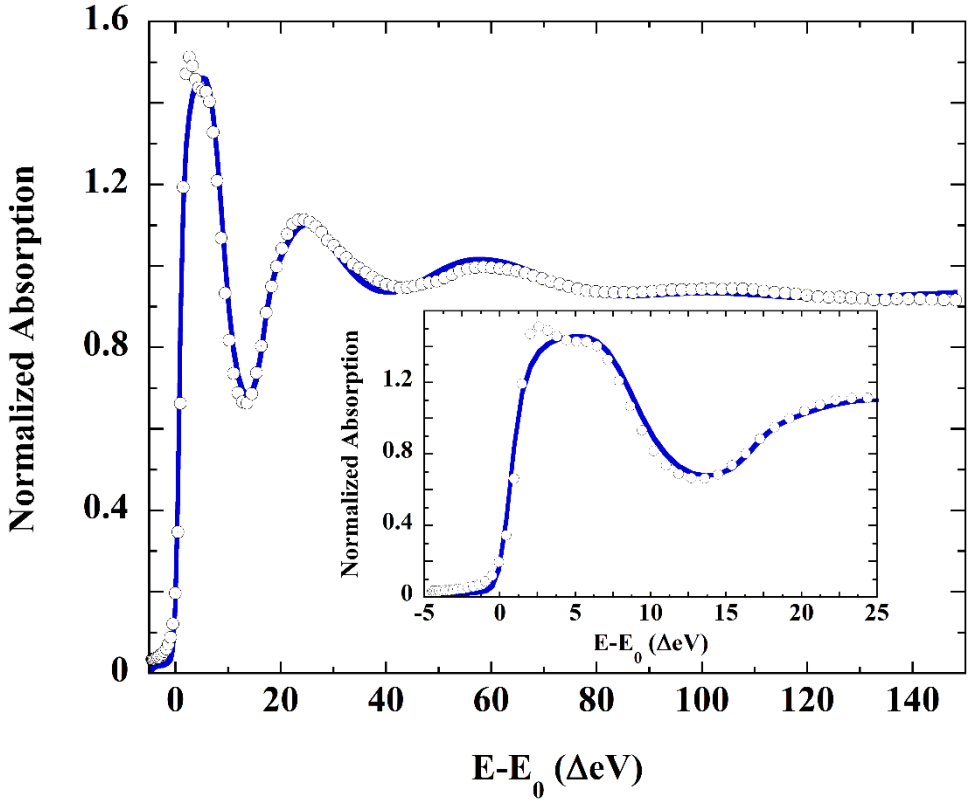

$$R_{th} = \frac{\sqrt{\sum_{i=1}^{m}(\sigma_i^{MD} - \sigma_i^{th})^2}}{m}$$

Spectrum calculated from the set of $R_{th} < 10^{-7}$ - $R_{sq} = 7.1$ - The R_{th} criterion selected 199 from the original 3190 frames.

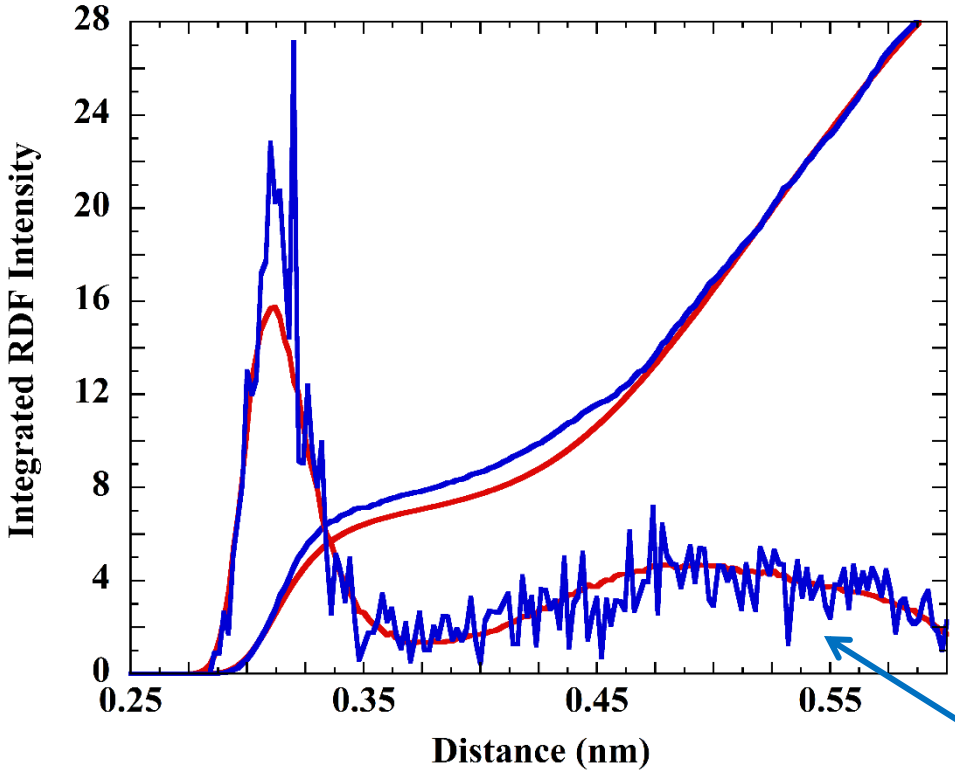

Cl-O g(r) obtained with R_{th} criterion

It seems that to improve the theory we need a further compression of the second hydration shell.

This effect is not easy to obtain with a two-body classical potential, because an alteration of the Cl-water or water-water interaction parameters would change the structure of the first hydration shell, as well

Nano materials – after a conversation with P. Frank and S.R. Bare

Is it possible to use a "MD"–like method for nano materials?

Au28

28 atoms of Au – each of them see a different environment – in principle we should have 28 different XAS spectra.

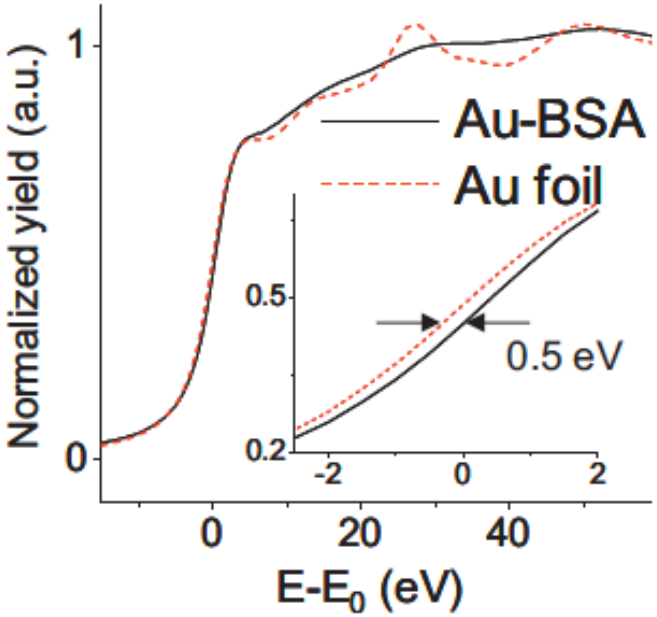

Au – L_3

$\Gamma_{c\text{-}h}$ = 5.4 eV

G.A. Simms, et al. J. Chem. Phys. 131, 214703 (2009)

The answer could be Yes

To generate thousands of clusters where the same type of atom experiences different environment – calculate the XAS for for each of those – sum and divide for the total number of used clusters – get the average

Trials must be done to check for the sensitivity and - **very important** - compare experiments with theory

MXAN and difference spectra

$$\Delta A(E,\Delta t) = f(\Delta t)[\mu_{ex}(E,\Delta t) - \mu_{gs}(E)]$$

$f(\Delta t)$ ← is the fractional population of the ex state at time delay Δt

To see (small) structural changes due to physical/chemical reasons in pump-probe experiments

Fields of application:

time resolved experiment
changes of chemical-physical and/or thermo-dynamical conditions
……

M. Benfatto et al. J. Phys. Chem. B (2006), 110 14035

The case of iron-(II)-tris-bypyridine $[Fe^{II}(byp)_3]^{2+}$

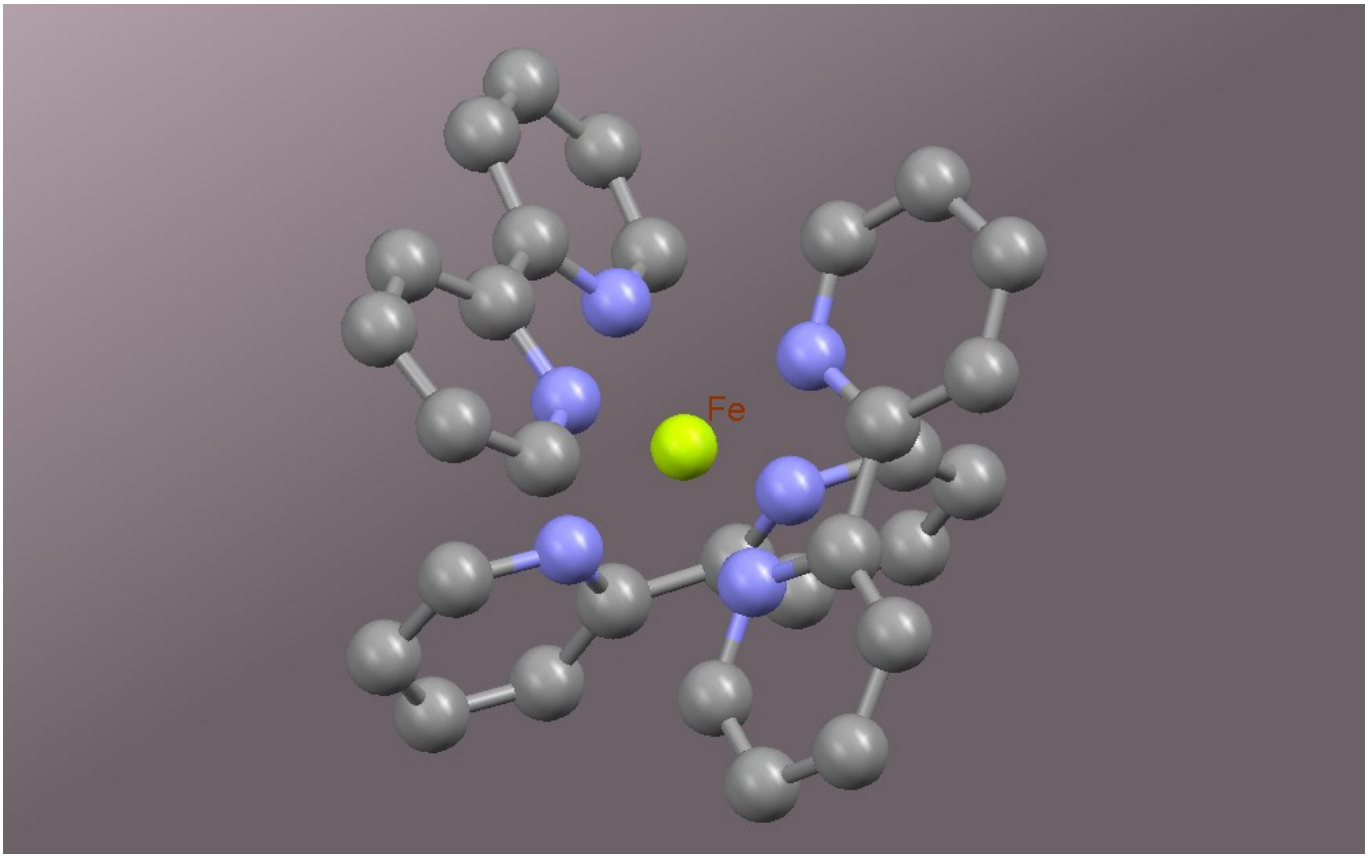

see the structural changes going from LS to HS state

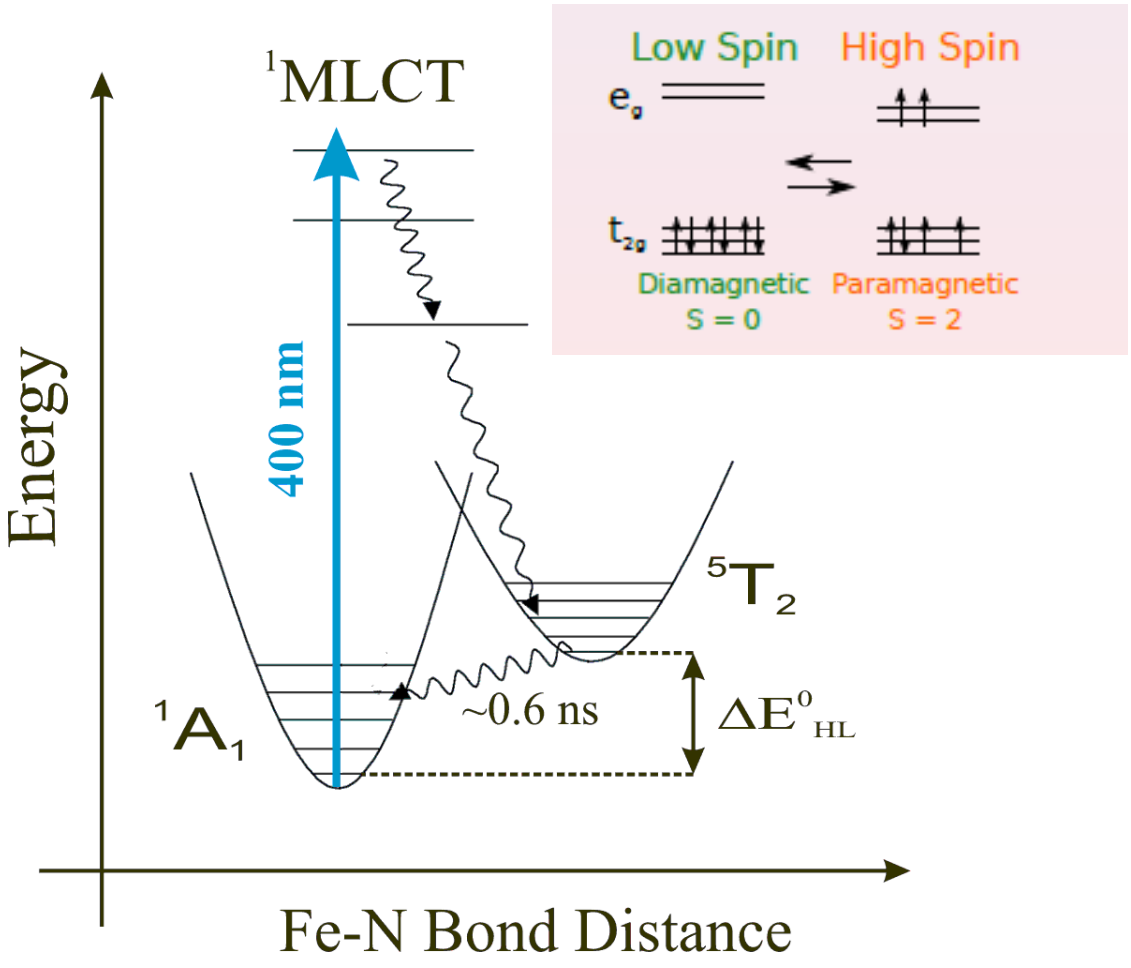

experiment done at the micro-XAS line of SLS by Chergui's group - pump-probe experiment in aqueous solution and room temperature

The detected signal is directly the quantity $\Delta A(E,\Delta t)$

experimental data

HS transient data at $\Delta t = 50$ ps

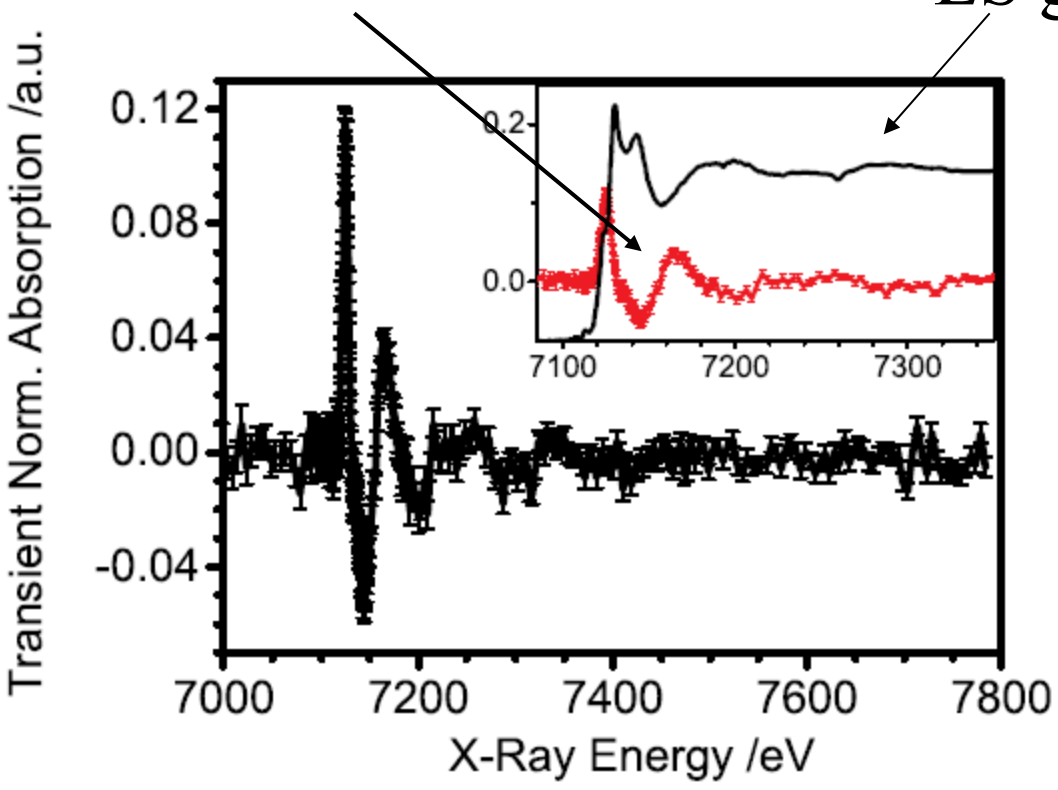

LS ground state fit

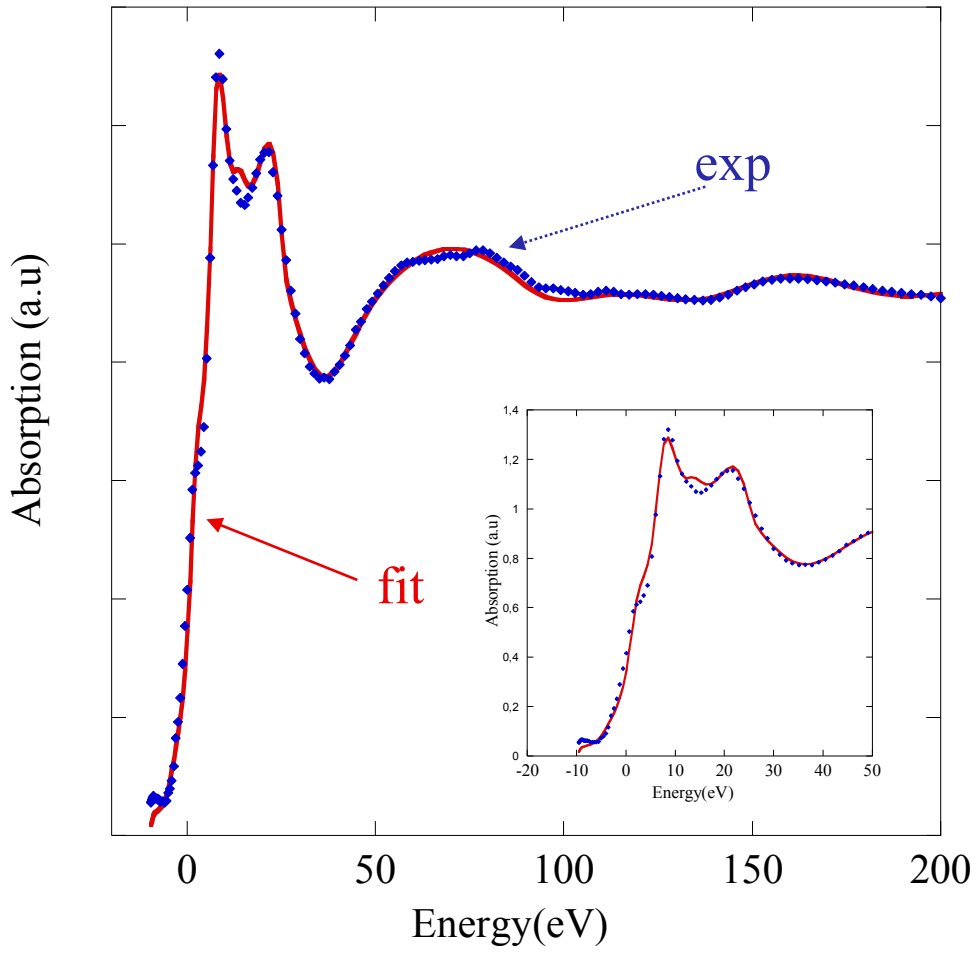

$R_{Fe\text{-}N} = 2.00 \pm 0.02$ Å

$R_{Fe\text{-}N} = 1.967 \pm 0.006$ Å (XRD)
$R_{Fe\text{-}N} = 1.99 \pm 0.02$ Å (DFT)

HS excited state fit by transient data

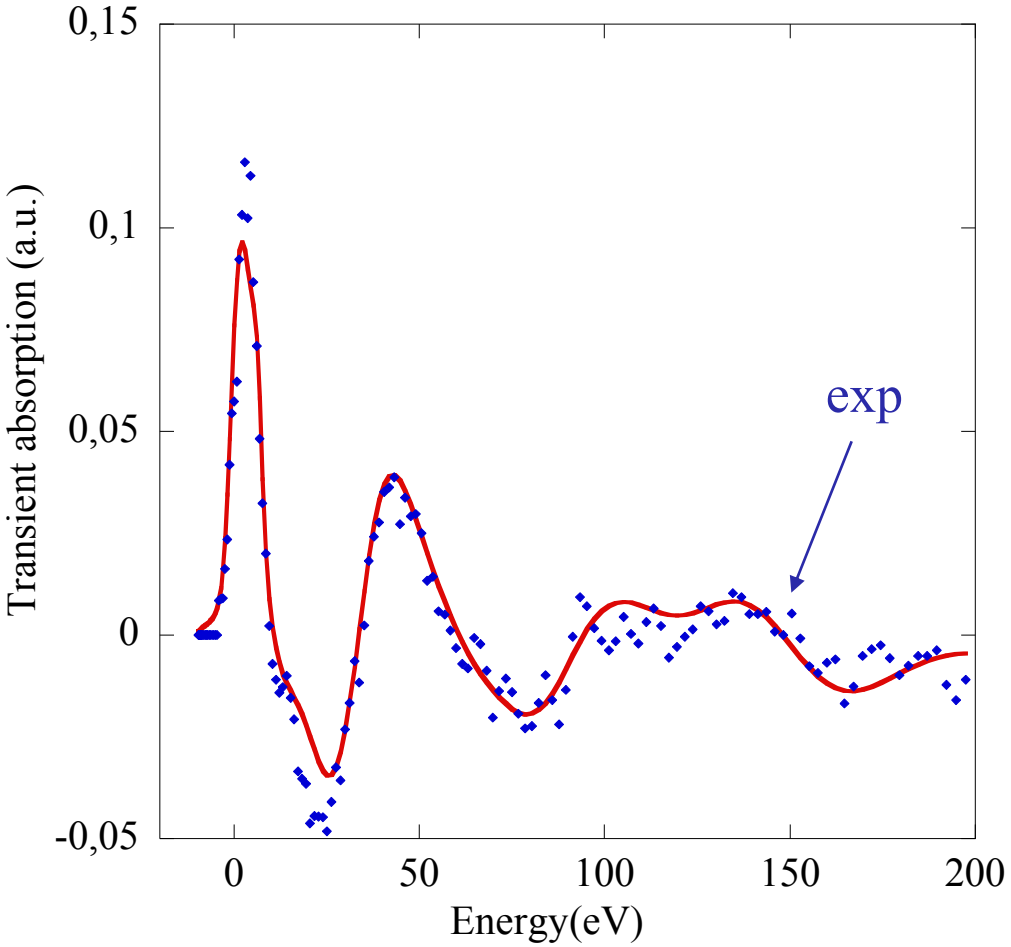

supposing a chemical shift $\Delta E = -2.5 \pm 0.5$ eV

$\Delta R_{Fe\text{-}N} = 0.20 \pm 0.05$ Å

DFT calculations indicate ~ 0.2 Å

W. Gawelda et al. PRL (2007) 98, 057401

Going to the fs time scale FEL experiment

iron-(II)-tris-bypyridine $[Fe^{II}(byp)_3]^{2+}$

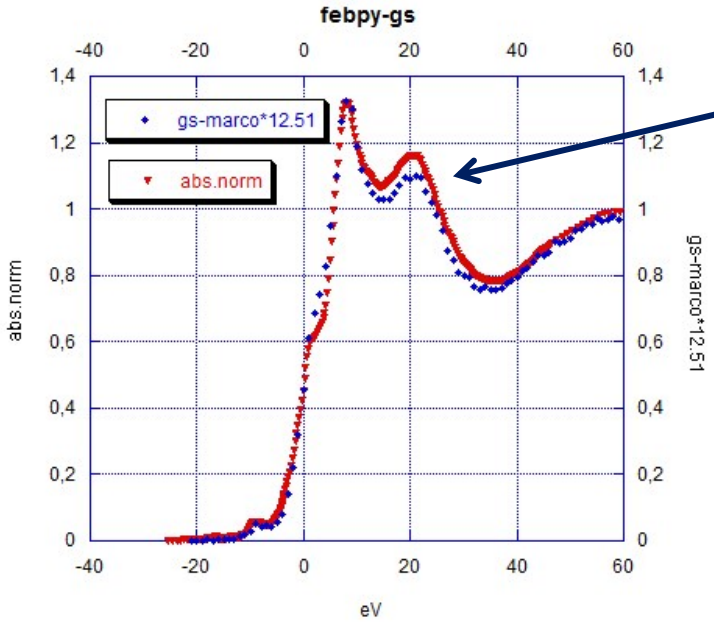

Exp data taken at LCLS

transient at 10 ps

MXAN fits of such data give almost the results previously obtained

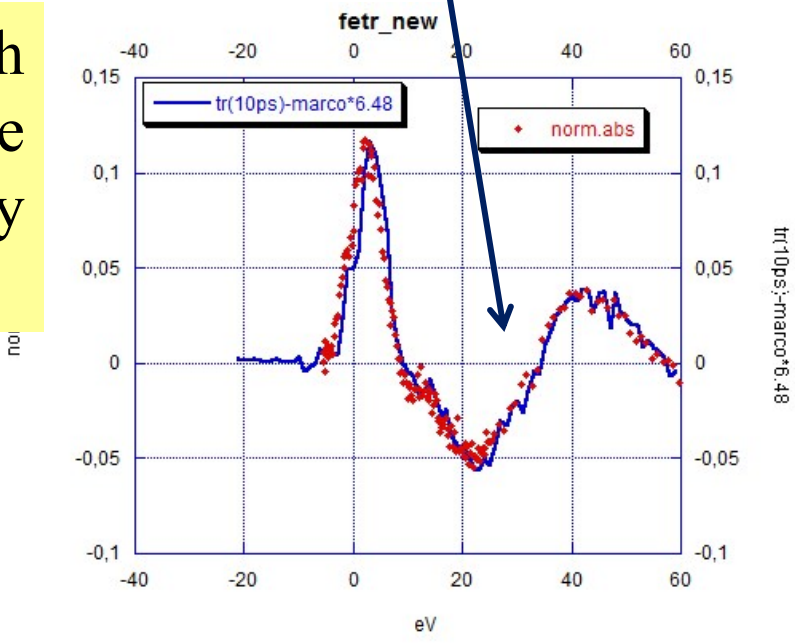

Experimental set-up at LCLS – time resolution ≈ 25 fs – the light is monochromatized by a double diamond (111) cristal – focus on sample ≈ 10 μm

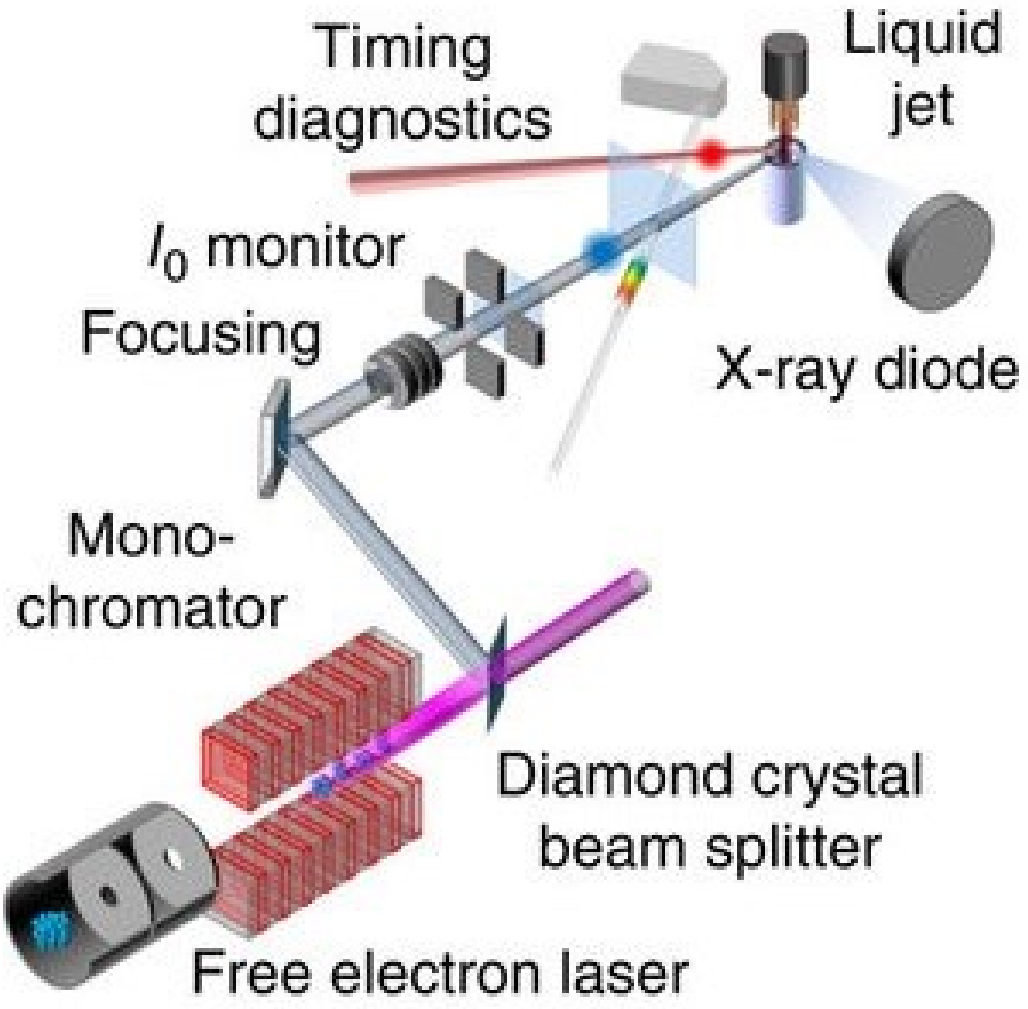

at the fs time scale it is impossible to take extedend experimental data – they must be taken at fixed energy

the transient data are taken as function of time but at fixed energy, in particular at 7120,7131,7144,7154,7162 eV

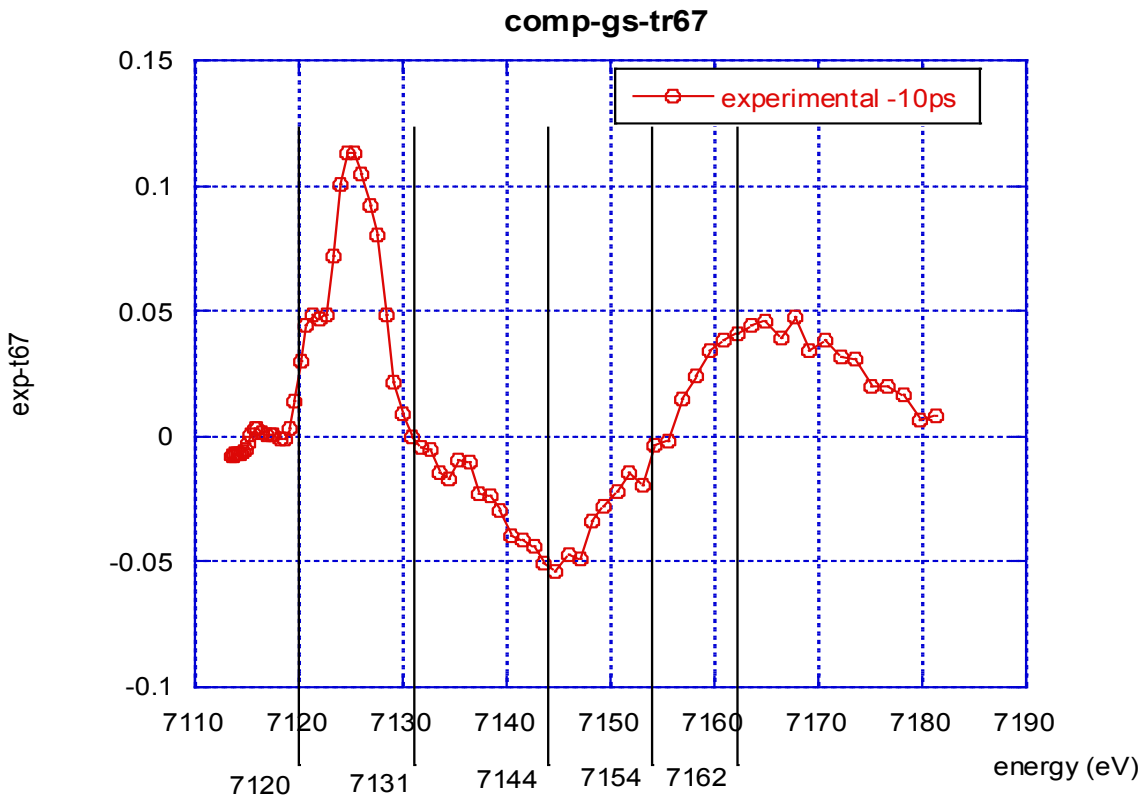

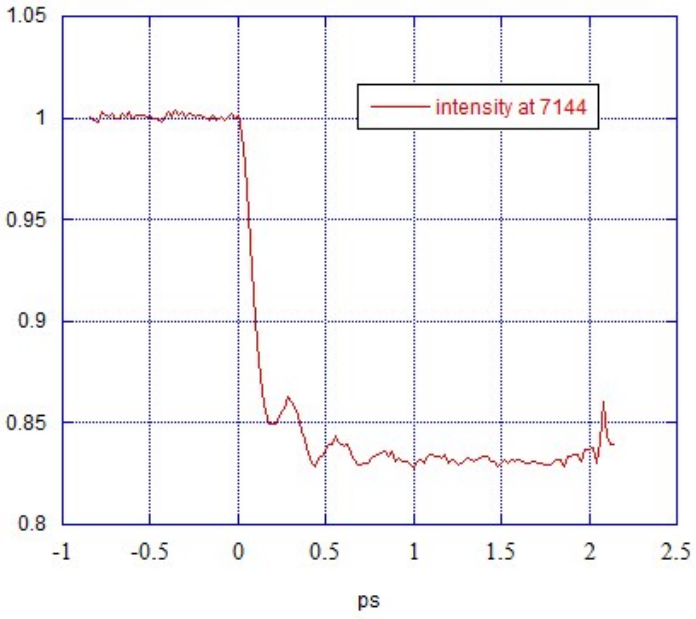

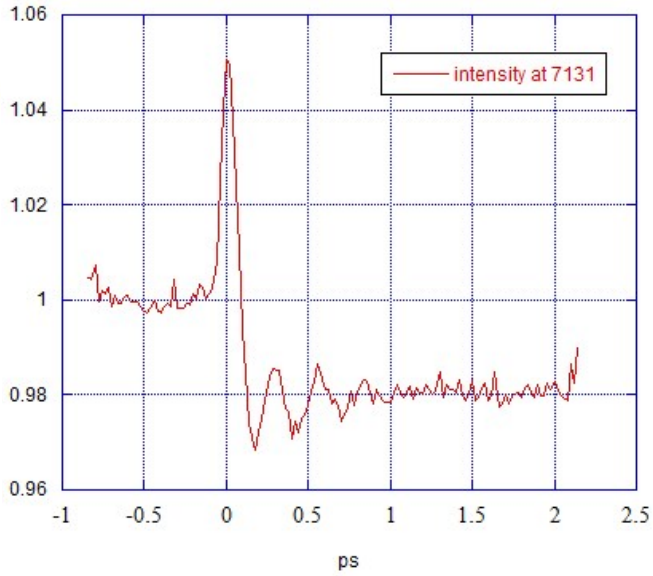

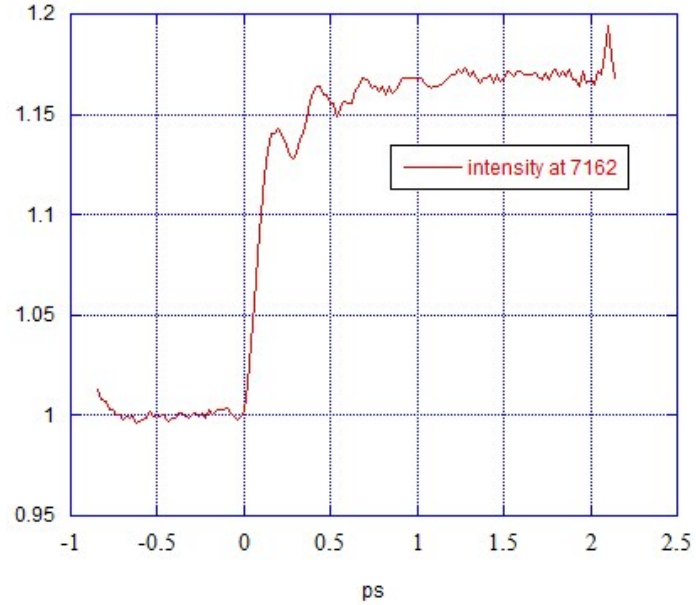

here the exp. data is the ratio

$$r(t,E) = S(t,E)/S_{GS}(E)$$

oscillations up to 2ps with a period of about 0.26 ps – the system is in the HS state after 2ps.

All data shows a rapid change within 30-200 fs followed by an oscillating phase up to 1-2ps. After this we reach the HS state.

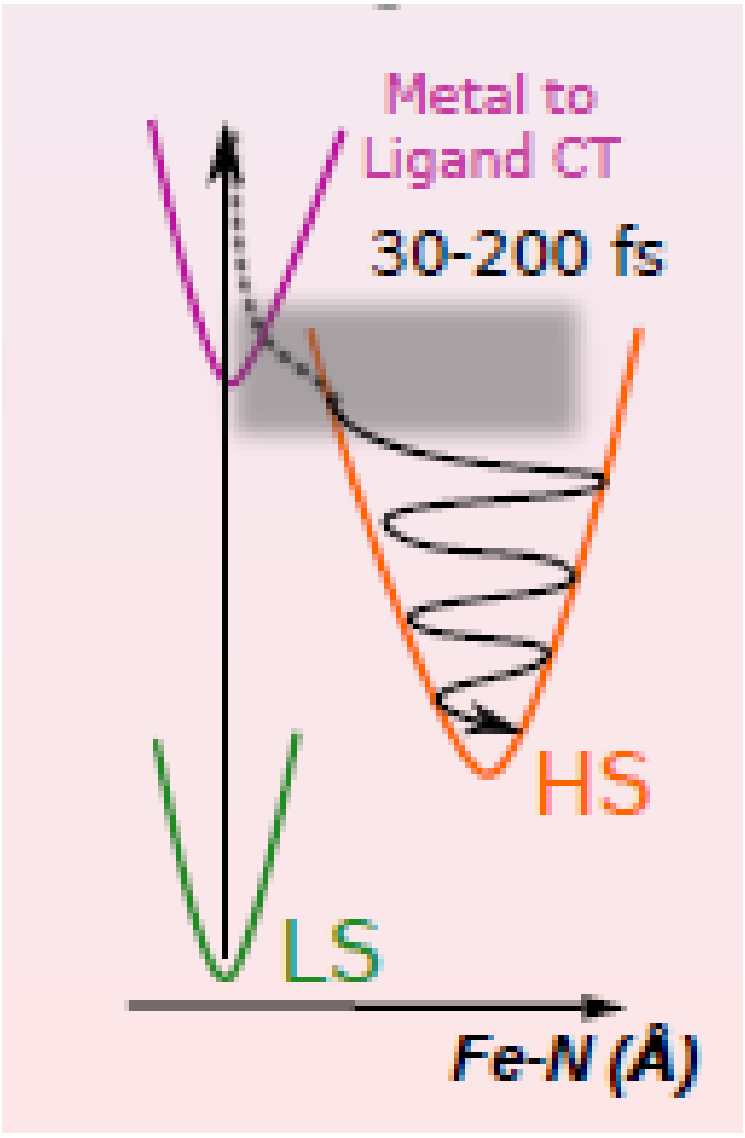

how to analyze these data?

We see how the calculated spectrum change as function of Fe-N distance

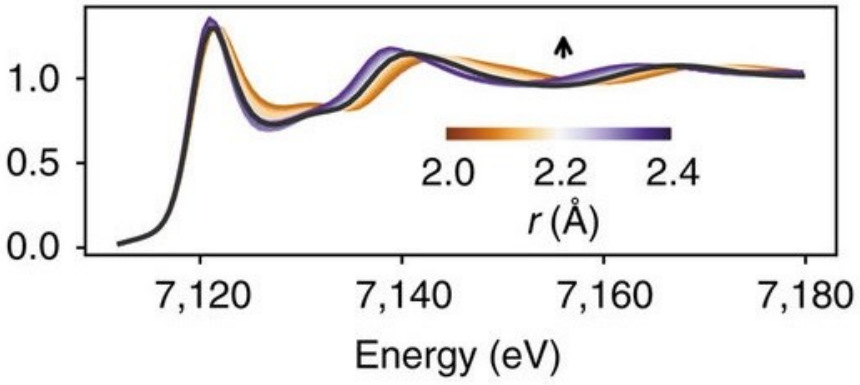

with these we see the dependence of the ratio signal at given energy for different chemical shifts – the reference is the calculation for Fe-N=2.0 Å and chemical shift -1.0 eV

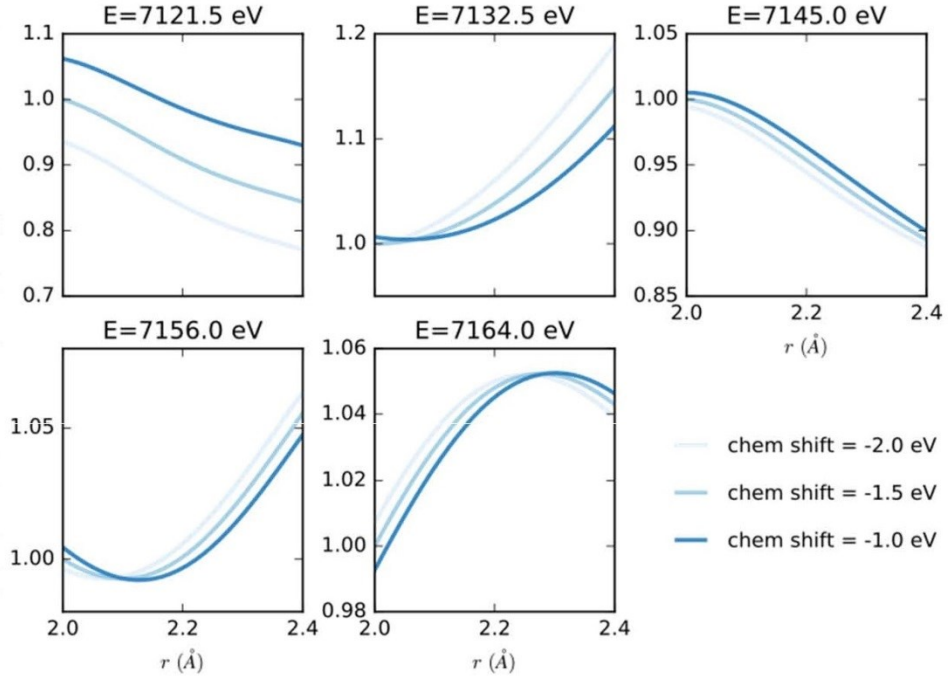

With these calculations we build the signal

$$I(t,E) = \int S(E,r)g(r,t)dr$$

where $S(E,r)$ is the calculated signal for given E and r - $g(r,t)$ is a time-dependent numeric distribution coming from the normal mode analysis of the vibrations of the rings. Some of them

a_{1g} 124.4 cm^{-1} breathing mode in phase Fe-N stretching with rigid bpy ligand

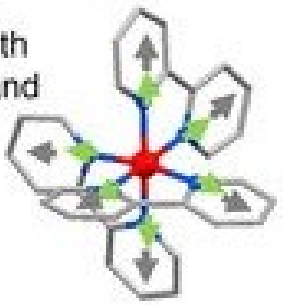

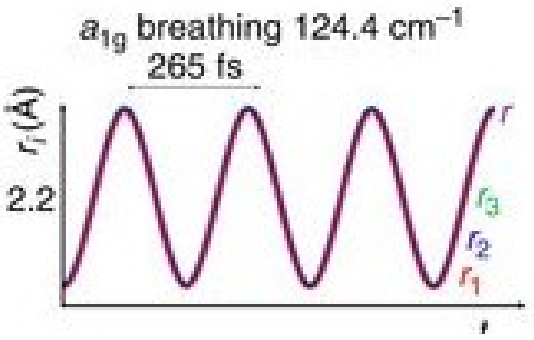

e_g 115.9 cm^{-1} out of phase Fe-N stretching

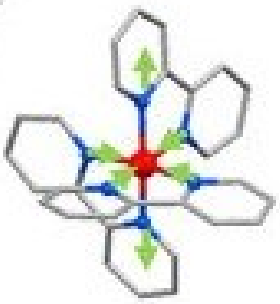

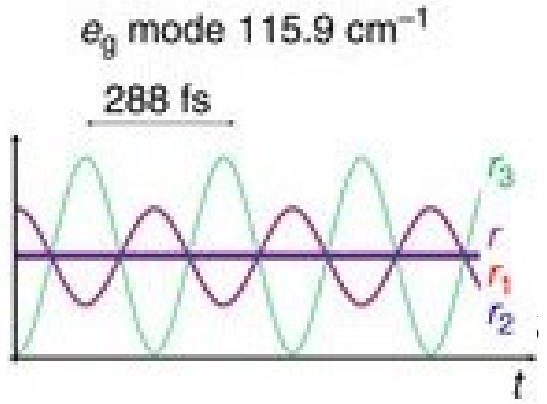

here we plot $\left[I(t, E_i) - I(E_i)_{off}\right]/I(E_i)_{off}$

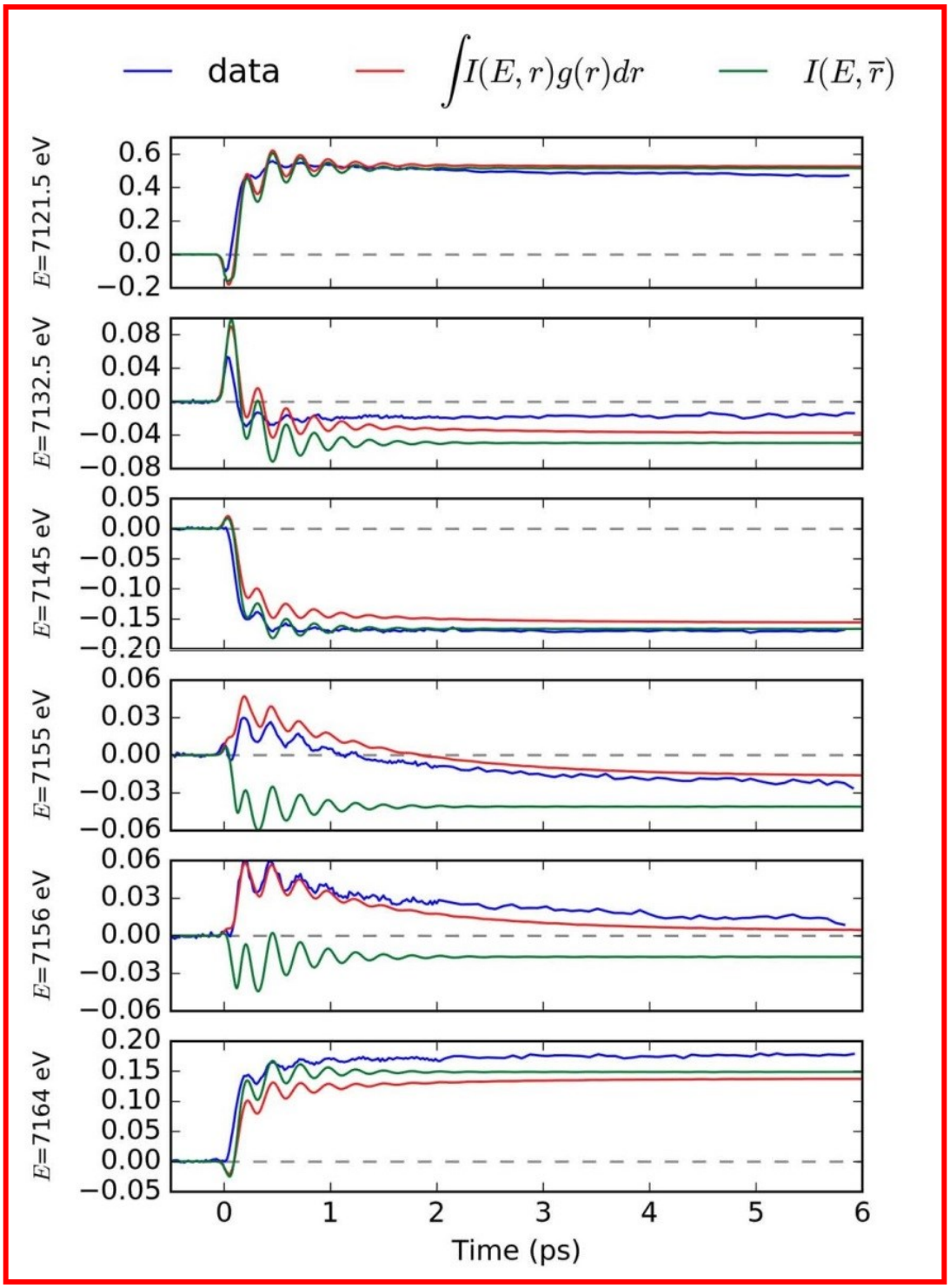

some conclusions

It is possible to fit the XANES energy range starting from the edge to obtain quantitative structural information

We can treat, although numerically, very disorder systems – possible application on nano-materials

Future: we are making a new version of MXAN to improve the speed, to have a better description of the EXC potential, to analyze the new type of data……..

Acknowledgments

- E.Pace - LNF – Frascati
- G. Chillemi – Cineca - Roma
- P. Frank - Stanford University and SSRL
- B. Hedmann and K.Hodgson - Stanford University and SSRL
- M. Cammarata – CNRS - Rennes
- M. Chergui - EPFL